

# Lawrence Berkeley National Laboratory

## Recent Work

### Title

STABILITY AND MECHANICAL PROPERTIES OF SOME METASTABLE AUSTENITIC STEELS

### Permalink

<https://escholarship.org/uc/item/9jx8k9zt>

### Authors

Bhandarkar, D.

Zackay, V.P.

Parker, E.R.

### Publication Date

1972-06-01

Submitted to Metallurgical  
Transactions

RECEIVED  
LAWRENCE  
RADIATION LABORATORY

LBL-125  
Preprint

DOCUMENTS SECTION

STABILITY AND MECHANICAL PROPERTIES  
OF SOME METASTABLE AUSTENITIC STEELS

D. Bhandarkar, V. F. Zackay, and E. R. Parker

June 1972

AEC Contract No. W-7405-eng-48



**For Reference**  
Not to be taken from this room

LBL-125  
c/1

## **DISCLAIMER**

This document was prepared as an account of work sponsored by the United States Government. While this document is believed to contain correct information, neither the United States Government nor any agency thereof, nor the Regents of the University of California, nor any of their employees, makes any warranty, express or implied, or assumes any legal responsibility for the accuracy, completeness, or usefulness of any information, apparatus, product, or process disclosed, or represents that its use would not infringe privately owned rights. Reference herein to any specific commercial product, process, or service by its trade name, trademark, manufacturer, or otherwise, does not necessarily constitute or imply its endorsement, recommendation, or favoring by the United States Government or any agency thereof, or the Regents of the University of California. The views and opinions of authors expressed herein do not necessarily state or reflect those of the United States Government or any agency thereof or the Regents of the University of California.

STABILITY AND MECHANICAL PROPERTIES  
OF SOME METASTABLE AUSTENITIC STEELS

\*D. Bhandarkar, V. F. Zackay, and E. R. Parker

ABSTRACT

The relation between austenite stability and the tensile properties, as affected by testing temperature and processing, was studied for a series of alloys of increasing compositional complexity, viz., the Fe-Ni, Fe-Ni-C and Fe-Ni-Cr-Mn-C systems. The "stress" and "strain induced" modes of transformation to martensite differed significantly in their influence on the shape of the stress-strain curve. Under certain testing conditions, unusually low yield strengths and high work hardening rates were observed in some of these alloys. Maxima in yield strengths were observed for all austenitic alloys containing carbon that were processed at deformation temperatures between 200° and 300°C. Evidence gleaned from electron microscopy and magnetic and mechanical testing suggested that the maxima were due to the formation of carbon atmospheres on dislocations during processing. The influence of austenite stability on the mechanical properties of steels, varied by systematic changes in test temperature (22° to -196°C), composition (8 pct, 12 pct, 16 pct and 21 pct Ni) and deformation temperature (25° to 450°C), was evaluated quantitatively.

---

\*D. Bhandarkar is Graduate Student, V. F. Zackay and E. R. Parker are Professors of Metallurgy, Inorganic Materials Research Division, Lawrence Berkeley Laboratory and Department of Materials Science and Engineering, College of Engineering; University of California, Berkeley, California.

## INTRODUCTION

The unusual combinations of strength, ductility and toughness that can be achieved in certain grades of commercial metastable austenitic stainless steels are known to depend strongly upon phase transformations occurring during processing or testing. The nature of these transformations and their influences on mechanical properties have been the subjects of active research for many years. It has been clearly established that both diffusion controlled reactions and martensitic transformations can occur in metastable steels and that the latter can be induced either by low stresses at temperatures near, but above the  $M_s$  temperature, or by stresses above the yield strength at temperatures well above the  $M_s$ . Martensite forming at low stresses is generally called "stress induced" martensite, and that requiring macroscopic plastic strain for initiation is called "strain induced". This distinction is somewhat arbitrary because it is the local state of stress that induces martensite formation in both cases.

Austenites transform into several types of martensite. The most common are the BCC and BCT ( $\alpha'$ ) martensites, which were the transformation products in the alloys involved in the studies reported herein. No evidence was found of the presence of the hexagonal ( $\epsilon$ ) martensite.

Within the last ten years renewed attention has been given to the effects of processing and testing variables on the stability of austenite. Utilization of this recently acquired knowledge has led to the development of a new class of ultra-high strength metastable austenitic steels. In these newer steels, the stability of the austenite with respect to

strain (or stress) has been shown to have a significant influence on strength (1-5), ductility (1-5), rates of work-hardening (3,4), fracture toughness (6-10) and low cycle fatigue behavior (11). The austenite stability is dependent upon the initial composition, the processing history, and the test environment (3-5).

One of the important processing steps is the prior deformation of the austenite (hereafter abbreviated as "PDA"). The primary purpose of such deformation is to raise the yield strength of the austenite to 200,000 psi or above. To achieve this objective, a large amount of deformation (70 pct to 80 pct) at a temperature between 200° and 450°C is required. Microstructural and chemical changes which alter austenite stability and mechanical properties can occur during this treatment. The first objective of this study was to identify these changes by systematically varying the chemical composition, the processing procedure and the testing conditions. The second objective was to relate the variations in austenite stability to the mechanical property changes.

Steels of widely differing compositions and processing histories were studied, including (a) a series of carbonless iron-nickel alloys of varying austenite stability; (b) a steel containing nickel and carbon without a strong carbide former, and (c) a series of steels of varying stability containing nickel, carbon, chromium, and manganese. The weaker carbonless Fe-Ni alloys were studied because the changes induced by processing were limited to those of structure. Chemical changes were additionally induced by processing in the Fe-Ni-C and the Fe-Ni-Cr-Mn-C steels. In the latter, the effect of a moderately strong carbide former (chromium) was studied.

EXPERIMENTAL PROCEDURE

Heats of approximately 15 pounds were melted in a helium atmosphere, cast in heavy copper molds and subsequently annealed in a neutral atmosphere for 3 days at 1100°C. The ingots were forged at 1100°C into plates 2-1/2" by 1/2" in cross section, which were subsequently reduced by rolling at 450°C to a thickness of 1/4". The plates were austenitized and brine quenched. The carbonless alloys were held at 1150°C for 1/2 hour and the carbon containing steels, at 1200°C for 2 hours. The final deformation (70 pct) was carried out at PDA temperatures of -120°, 25°, 100°, 150°, 200°, 250°, 300° and 450°C (except where otherwise noted). Preheated rolls were used for PDA temperatures of 100°C and above and temperature control was maintained by returning the pieces to the furnace between passes to reestablish temperature equilibrium. The heated pieces were water quenched after the final pass. The compositions of the alloys are given in Table I.

Sheet tensile specimens having a 1 inch gage length, a thickness of 0.05 inch, and a test section width of 0.125 inch, were ground from the processed sheets. The specimens were loaded through aligning pins in the wide ends of the specimens. The total elongation was measured between small indentations. A yield point occurred in many cases, and the yield stress was taken as the upper yield point. When there was no drop in load, the 0.1 percent offset method was used to obtain the yield strength. The strain rate employed was 0.04 per minute; for test temperatures below room temperature, the specimen was immersed in a temperature controlled liquid.

TABLE I. CHEMICAL COMPOSITIONS OF ALLOYS

Designation	Compositions, Wt Pct			
	C	Ni	Cr	Mn
34N	< 0.010	33.7	-	-
38N	< 0.010	37.8	-	-
CN28	0.294	28.0	-	0.5
CN8Cr	0.325	8.0	9.0	2.0
CN12Cr	0.290	12.0	9.0	2.0
CN16Cr	0.292	16.0	9.0	2.0
CN21Cr	0.287	21.4	9.0	2.0



The amount of transformation that occurred during testing was determined quantitatively by measuring the saturation magnetization of tensile specimens before and during testing at various temperatures. The readings were converted to volume percentage of martensite, with corrections being made for the influence of the alloying elements (12,13). This method could not be used for the ferromagnetic carbonless high nickel alloys. For these alloys the volume percent martensite was estimated by metallography.

Thin foils for electron microscopy were prepared by a jet electropolishing technique using a mixture of one part of perchloric acid to four parts of acetic acid. A Siemens Elmiskop 1 electron microscope operated at 100 kV was used for the transmission microscopy.

The approximate  $M_s$  and  $M_d$  temperatures for all alloys were determined either by metallographic, magnetic, or electrical resistivity techniques and are listed in Table II. The thermomechanical history of each alloy is indicated in the Table; transformation temperatures sometimes change with variations in processing.

TABLE II. ESTIMATED  $M_s$  AND  $M_d$  TEMPERATURES OF ALLOYS

Designation	Thermomechanical Process	Estimation of $M_s$		Estimation of $M_d$	
		$M_s$ , °C	Technique Used	$M_d$ , °C	Technique Used
34N	70% PDA at temperatures between 22°C and 450°C	-85	Resistivity	10-22	Tension test*
38N	70% PDA at temperatures between 22°C and 450°C	<-196	Resistivity	About -150°C	Tension test
CN28	70% PDA at temperatures between 22°C and 450°C	-68	Resistivity	About 25°C	Tension test
CN8Cr	For estimation of $M_s$ only: 70% PDA at temperatures between 22°C and 450°C	<-196	Magnetic measurements	150°C	70% deformation by rolling**
CN12Cr	Same as above	<-196	Magnetic measurements	22°C	Tension Test
CN16Cr	Same as above	<-196	Magnetic measurements	About -120°C	70% deformation by rolling
CN21Cr	Same as above	<-196	Magnetic measurements	About -196°C	Tension test

\*The alloy after thermomechanical processing was tested in tension at various temperatures and the  $M_d$  was estimated as the temperature above which no deformation induced martensite formed.

\*\*The alloy was examined after 70% PDA at several temperatures and the  $M_d$  was estimated as that above which no deformation induced martensite formed.

RESULTS AND DISCUSSION

Carbonless Iron-Nickel Alloys

In the absence of carbon, only substructure and grain structure changes were induced by the PDA in metastable austenite. The Fe-Ni alloy, 38N, whose  $M_s$  and  $M_d$  were below the lowest PDA temperature ( $-120^\circ\text{C}$ ) was first investigated. The mechanical properties of this stable alloy were established to provide a basis for comparison with the more complex and less stable alloys subsequently investigated.

The effects of the PDA temperature on the room temperature and  $-196^\circ\text{C}$  yield strengths of alloy 38N are shown in Fig. 1(a). Linear variations of the yield strengths with PDA temperature were obtained; the effect of varying the PDA temperature was small. Characteristically, the room temperature elongation values were small and the rates of work hardening were low.

The effects of the PDA temperature on the carbon-free alloy, 34N, which was stable above room temperature but unstable at cryogenic temperatures, was determined next. The yield strengths are shown in Fig. 1(b) as a function of the PDA temperature. The yield strengths rose rapidly below the  $M_d$ , which was found to be between  $10^\circ$  and  $22^\circ\text{C}$ . The  $M_s$  was about  $-85^\circ\text{C}$ . Above the  $M_d$ , the variation of the yield strengths with the PDA temperature was nearly identical to that observed for the stable alloy, 38N. Martensite was produced during the rolling operations below the  $M_d$ . Its presence raised the room temperature yield strength. The martensite (both athermal and deformation induced) produced during processing is clearly visible in Fig. 2. The before-testing microstructure of the alloy rolled at  $-120^\circ\text{C}$  is shown in Fig. 2(a) and the

athermal martensite produced during cooling to the test temperature after rolling above the  $M_d$  is shown in Fig. 2(b).

The behavior of the less stable alloy, 34N, was significantly different from that of alloy 38N with respect to testing temperature, as can be seen by comparing Fig. 1(b) with Fig. 1(a). With a change in test temperature from 22° to -196°C there was a sharp drop in the yield strength (about 22 pct) of alloy 34N. The decrease in yield strength at the lower test temperature was observed above a PDA temperature of about -100°C; at lower PDA temperatures the alloy was stronger at -196°C than it was at 22°C. A drop in yield strength at low test temperatures has been observed by previous investigators. This phenomenon has been attributed to the stress induced formation of martensite (14-23). Yielding occurs as a consequence of the phase transformation when the critical stress for transformation is less than that required for the initiation of slip in austenite. Certain features of the engineering stress-strain curves of specimens tested at both room and cryogenic temperatures lend support to this view.

Typical stress-strain curves of specimens tested at both 22° and -196°C for alloy 34N, deformed 70 percent at a PDA temperature of 450°C, are shown in Fig. 3. The stress-strain curve of the specimen tested at room temperature is characteristic of that of a stable cold-worked austenitic steel, i.e., a high yield strength, a low rate of work-hardening, and an elongation of about 10 percent. The absence of serrations in the stress-strain curves and the low work-hardening rate are consistent with metallographic observations, which revealed that no martensite was present in the specimens after testing. Stress-strain

curves of specimens deformed at all PDA temperatures above  $M_d$  and tested at room temperature were similar to the 22°C curve shown in Fig. 3.

The stress-strain curve for the specimen tested at -196°C is different in several respects. As shown in Fig. 3, the yielding of the austenite occurred at a lower stress than that observed at 22°C. The rate of work hardening was high, and the elongation was nearly twice that of the specimen tested at room temperature. The low elastic limit observed in the test at -196°C was attributed to the formation of martensite nucleated by local stresses at loads well below the elastic limit of stable austenite at the test temperature. The high rate of strain hardening in the plastic strain range is strong evidence of "strain induced" martensite formation. Thus both "stress induced" and "strain induced" martensite formed in this specimen during the test. Also, a metallographic examination of the unstrained end of the test specimen revealed that about 70 percent of athermal martensite was present prior to tensile testing (Fig. 2(b)). After testing, the alloy in the gage length was almost completely martensitic. Stress-strain curves of specimens deformed at all PDA temperatures above the  $M_d$  and tested at -196°C were similar to the one shown in Fig. 3.

The mechanical properties observed can be explained if the deformation mechanisms include strains due to the formation of "stress induced" martensite. In recent years a number of investigators have emphasized the importance of this mechanism of plastic flow in metastable austenitic steels, especially at temperatures near the  $M_s$ . Angel (17), in particular, made detailed studies of the yield behavior of annealed metastable steels at temperatures ranging from above the  $M_d$  to below

the  $M_s$ . Some of his conclusions were as follows: at temperatures above the  $M_d$  the yielding is entirely by slip of the austenite; below the  $M_d$  and above the  $M_s$ , two other mechanisms of flow are likely to be operative, either singly or together, viz., the "strain induced" and the "stress induced" modes of the transformation of austenite to martensite; and, finally, below the  $M_s$  the stress induced mode of the transformation is dominant. Between the  $M_d$  and the  $M_s$ , Angel stressed that the two modes of yielding mentioned above were competitive, the dominant one being determined by the test temperature, i.e., the strain induced mode being favored near the  $M_d$  and the stress induced mode being favored near the  $M_s$ .

Fahr has shown in a recent study that certain metastable austenitic stainless steels of low stability have low yield strengths and high rates of work hardening (5). He concluded that these properties are characteristic of an alloy in which the formation of martensite is stress induced. In unpublished work, Fahr observed yield-to-tensile strength ratios as low as one-quarter (23). As illustrated in Fig. 3, the total elongation of a steel undergoing a stress induced transformation may be nearly twice that of a similar, but stable, steel. It will be shown in a later section, however, that metastable steels containing carbon may have low ductility because of the brittleness of the stress induced martensite. Thermomechanical treatments which tend to stabilize austenite favor the strain induced transformation, while those which destabilize the austenite favor the stress induced mode.

The variation of the yield strength with the PDA temperature for alloy 34N is shown for test temperatures of  $-78^{\circ}\text{C}$  and  $22^{\circ}\text{C}$  in Fig. 4.

The mechanical properties between the  $M_d$  (approximately 15°C) and the  $M_s$  (-85°C) are consistent with the observations of Angel, namely, that either or both modes of the transformation may occur when tensile tests are made in this temperature range. Both modes did occur in specimens having PDA temperatures of 25°C and 100°C, when they were tested at -78°C (Fig. 4). Metallographic studies of the specimen having a PDA temperature of 25°C confirmed the fact that no martensite was present before testing, but that large amounts existed after testing.

As shown in Fig. 4, the -78°C yield strength increased with increasing PDA temperature, rising to a value greater than that measured at room temperature. This behavior showed that processing at higher PDA temperatures had stabilized the austenite, thereby favoring the strain induced over the stress induced transformation. The principal features of the stress-strain curves for alloy 34N are shown in Fig. 5. As a consequence of the stability change, the extent of the Lüders strain increased with the PDA temperature, the rate of strain hardening decreased, and the total elongation became larger.

A direct measurement of the stability change produced by varying the PDA temperature was made by determining the  $M_d$  for two extreme PDA temperatures, viz., 25°C and 450°C. The  $M_d$ 's, estimated by means of metallographic and x-ray diffraction techniques of the strained tensile specimens, were found to differ by about ten degrees; the specimen with the PDA temperature of 450°C having the lower  $M_d$ . This result supports the view that the stability, the mode of transformation, and the mechanical properties of a carbonless austenitic alloy can be changed by thermo-mechanical processing. In carbon containing steels chemical as well as

structural changes are produced by processing, with similar, but larger, effects on stability and mechanical properties. These are discussed in the next section.

#### Iron-Nickel-Carbon and Iron-Nickel-Chromium-Carbon Steels

A series of steels was prepared to investigate the interrelationships between processing, austenite stability and mechanical properties. The principal variables were the composition of the steel and the PDA temperature. The amount of the deformation was held constant. (The effects of the amount of deformation on the properties of this class of steels has been reported in detail by Fahr (5,23)).

The amounts of nickel, manganese and carbon in the first steel of this series, CN28, were adjusted so that the  $M_d$  was in the same temperature range as that of the carbon-free steel, 34N. The nickel contents of the remaining steels of the series were varied to cause a systematic change in austenite stability, as shown in Table II. The levels of carbon, manganese, and chromium were maintained constant. The relation between structure and properties of the iron-nickel-carbon steel, for several processing and testing conditions will be discussed first.

The variation of yield strength with the PDA temperature for steel CN28 (70 percent deformation) is shown in Fig. 6, for two test temperatures. The  $M_s$  for this steel after processing was estimated to be  $-68^\circ\text{C}$  and the  $M_d$  was estimated to be about  $25^\circ\text{C}$ . At PDA temperatures below  $M_d$ , strain induced martensite was formed. The high yield strengths obtained at the lower PDA temperatures reflected the duplex nature of the microstructure. The behavior was similar to that of alloy 34N, except that



the overall strength level was higher because of the greater hardness of the martensite.

For PDA temperatures above the  $M_d$ , the yield strength varied in a different manner from that of the carbonless iron-nickel alloys, as can be seen by comparing Fig. 1(b) with Fig. 6. A broad maximum was found between 200°C and 300°C for the carbon containing steel, CN28. A similar maximum was also evident at the -78°C test temperature even though the strength level was almost 100,000 psi below that found at 22°C. The lower yield strength at the lower test temperature can be attributed to the stress induced formation of martensite.

Maxima in yield strength of the kind shown in Fig. 6 appeared to be unique to alloys containing carbon; they were never observed in carbon-free alloys. Yield strength maxima were obtained with steels of widely differing stabilities. The variation of the room temperature yield strength with PDA temperature for steels CN8Cr, CN12Cr and CN21Cr (whose  $M_d$ 's were 150°, 22°, and -196°C respectively) are shown in Fig. 7. These steels were processed in a similar manner; they differed primarily in nickel content. When tested at 22°C, they exhibited maxima varying slightly from each other in height and position. Similar peaks were also found when tests were made at -78°C, as shown in Fig. 8. The low -78°C yield strengths of CN8Cr, the least stable steel, were due to the stress induced martensitic transformation.

Other investigators who have made elevated temperature tensile tests on annealed austenitic steels have found peaks in the yield strength vs temperature curves, and such peaks have also been found in

martensitic steels (24-31). Such maxima are usually attributed to the formation of carbon atmospheres or precipitates on the dislocations. Parker and Hazlett, as well as others, have concluded that clusters and precipitates formed in this manner can lead to small but significant increases in yield strength (25,27,32). In principle, it is also possible that discrete precipitates of iron or chromium carbides might form during the PDA, but precipitation seems improbable at the low temperatures associated with the peaks. Transmission electron microscopy of specimens exhibiting the peaks provided no evidence that precipitate particles had formed. The structure of steel CN12Cr, deformed 70 percent at 300°C, is shown in Fig. 9, with both bright and dark field illumination. The structure was characterized by a high dislocation density, a strong texture with a  $(110)_\gamma$  orientation, and the presence of deformation twins. The latter were positively identified by a reversal of contrast in a dark field image of the  $(\bar{1}\bar{1}1)_\gamma$  twin spot (see Fig. 9(b)). Additional studies were made on specimens aged for various times (2, 5, and 10 days) at the various PDA temperatures. If carbides existed after the PDA treatments, but whose sizes were below the resolution of the detection technique (estimated to be about 20 Å), they should then have grown with aging and become visible. Again no carbide particles could be detected.

The variation of the room temperature yield strength with the PDA temperature for steel CN8Cr, shown in Fig. 7, exhibited a well defined peak in yield strength at a PDA temperature of approximately 250°C. The amounts of martensite, as determined by magnetic saturation values

for the same steel strained in tension one and two percent at 22°C, are shown as a function of the PDA temperature in Fig. 10. Maxima in the percentage of martensite occurred at a PDA temperature of 250°C. At strains somewhat larger than two percent, the amount of martensite was greater and the peaks were less pronounced. The maxima in volume fraction of martensite vs PDA temperature curves indicate a minimum in austenite stability at the PDA temperature corresponding to the peak in the curve.

The correspondence of the decreased austenite stability with the peak in yield strength in the same PDA temperature range indicates that the yield strength peak is a consequence of chemical changes that occurred in the austenite during the PDA. While the combined electron microscopy, magnetic and mechanical property evidence is consistent with the concept that these chemical changes are associated with the various states of aggregation of carbon in the austenite lattice, conclusive evidence that this is so is not yet available. The lower yield strengths associated with PDA temperatures above 250°C are thought to be a consequence of smaller amounts of carbon clustering around dislocations because of the higher solubility of carbon in austenite. Conversely, at PDA temperatures below 250°C, the mobility of the carbon is considered to be too low to form atmospheres during the time required for deformation.

#### Stability Criteria

In the previous section, the changes in austenite stability (with respect to athermal and deformation types of transformations) produced by variations in chemical composition or processing have been described in qualitative terms. There have been attempts to establish quantitative

measures of stability (3,17), which are relevant to the present investigation. In the following discussion two criteria will be compared using data obtained on the carbon containing steels.

Angel, in a study of austenitic 18-8 type stainless steels, found that an equation of the type

$$\ln \frac{f}{1-f} = A \ln \epsilon + k$$

best fitted his data. In this equation,  $f = \frac{V_{\alpha}}{V_T}$  where  $V_{\alpha}$  is the volume of austenite transformed to martensite,  $V_T$  is the maximum amount of martensite that can form by plastic deformation,  $\epsilon$  is the true strain, and  $A$  and  $k$  are constants. The equation is of the log autocatalytic type given by Austin and Rickett (33), with the strain parameter replacing time. Angel found that when the curves of  $\frac{f}{1-f}$  vs  $\epsilon$  were plotted on a log/log scale, a series of virtually straight lines was obtained. The slope,  $A$ , was approximately equal to 3 and was independent of chemical composition and temperature. The constant,  $k$ , however, varied with both these factors. In contrast to the present study, the range of stabilities of the alloys used in Angel's work was small ( $M_d$  from  $-15^{\circ}$  to  $38^{\circ}\text{C}$ ;  $M_s \approx -180^{\circ}\text{C}$ ) and the alloying elements in his steels were limited to a relatively narrow range (Ni 4-9 pct, Cr 15-19 pct, C 0.06-0.24 pct). Another difference was the fact that all the alloys of the present study were severely deformed and therefore had much higher yield strengths than those of Angel's.

Gerberich, et al, have suggested that the volume fraction of martensite,  $V_{\alpha}$ , produced during a tensile test varies as

$$V_{\alpha} = m \epsilon^{\frac{1}{2}}$$

where  $m$  is a constant for a given set of test conditions and  $\epsilon$  is the conventional strain (3). The transformation coefficient,  $m$ , was found to be a useful index of austenite stability, with higher values of  $m$  indicating lower degrees of stability. The value of  $m$  was obtained by plotting  $V_\alpha$  vs  $\epsilon^{1/2}$  and fitting the best straight line to the data. The correlations between Lüders strain, elongation at fracture, and the stability coefficient are shown in Fig. 11 for a large group of alloys of widely varying composition and processing histories. Gerberich showed that for a wide variety of steels and processing conditions, the stability coefficient,  $m$ , was a useful index of austenite stability for steels having large amounts of PDA. The value of  $m$  is necessarily zero when the test temperature is at or above the  $M_d$  temperature. For temperatures well below the  $M_d$ ,  $m$  was found to be as high as 3.5.

Typical experimental data for steel CN8Cr, deformed 70 percent at 450°C, are shown in Fig. 12 for test temperatures of 22°, -78° and -196°C. Curves representing the relationships of  $V_\alpha$  and  $\epsilon$  suggested by Angel and Gerberich, et al, are also shown in Fig. 12, as are the experimentally determined points. For the Angel criterion all calculations were based on true strain, whereas engineering strain was used for the Gerberich function. It is evident that neither criterion accurately predicted the data over the complete range of strains. For the room temperature test, the data at low strains seemed to be in accord with the Angel model, but at higher strains (and at the lower test temperatures), the Gerberich formulation seemed to be better.

### Stability and Mechanical Properties

A reliable stability index for high strength metastable austenitic steels would permit predictions to be made of the effect of composition and processing conditions on mechanical properties. In the ensuing discussion, the Gerberich relationship will be used as a stability criterion to describe the properties of several steels.

The engineering stress-strain curves at several testing temperatures are shown in Fig. 13 for the CN8Cr steel deformed 70 percent at 450°C. The  $m$  values are also shown. The stress-strain curve obtained at 22°C exhibited a well defined Lüders strain, a low work hardening rate and an elongation at fracture of 20 pct corresponding to an  $m$  value of 1.85, as shown in Fig. 11(a) and (b). The relatively low rate of work hardening is a consequence of the comparatively low rate of formation of martensite with strain, as can be seen from Fig. 12(a).

At the test temperature of -78°C, both the stability and the shape of the stress-strain curve are quite different, relative to those at room temperature, as can be seen in Fig. 12(b) and Fig. 13. The yield strength was lower by about 60,000 psi, the Lüders band was well defined, the rate of work hardening was much higher, and the elongation at fracture was about one-half of the room temperature value. These features are consistent with the change in stability as reflected by the  $m$  value, 2.37 (Fig. 11). Of particular interest are the low yield strength and the high rate of work hardening. These features are characteristic of an alloy undergoing a stress induced phase transformation. The large amount of martensite produced at low strains is another characteristic feature of this type of transformation. At a strain of 0.02, about half

the austenite had been transformed to martensite in the  $-78^{\circ}\text{C}$  test. In the specimen tested at  $22^{\circ}\text{C}$ , less than 10 percent of the austenite had transformed for the same strain.

The stress-strain curve and transformation behavior of the specimen tested at  $-196^{\circ}\text{C}$  are similar in kind but different in detail from those observed at  $-78^{\circ}\text{C}$ . The yield strength was somewhat higher (by about 25,000 psi) a reflection of the increased strength of austenite at the lower temperature. The rate of work hardening, the extent of the Lüders strain and the elongation to fracture were similar to those observed at  $-78^{\circ}\text{C}$  as was the rate of formation of strain induced martensite at strains above about 0.05. The latter fact was observed when the volume fraction of martensite vs strain curves for the two test temperatures were replotted after making a correction of 0.15 for the extra stress induced martensite that formed at  $-78^{\circ}\text{C}$ . The two curves approximately coincide as shown in Fig. 12(d). The estimated value of  $m$  is 2.37 and the Gerberich relation can be written as  $V_{\alpha} - V_0 = m\epsilon^{1/2}$  where  $V_0$  is the volume fraction of stress induced martensite that formed just after the yield point. It is well known that the modulus and the yield strength of FCC metals increase with decreasing temperature (34,35). The increased resistance to flow should reduce the amount of stress induced martensite. Consistent with this explanation is the fact that the flow stress is higher at  $-196^{\circ}\text{C}$  than at  $-78^{\circ}\text{C}$ , as shown in Fig. 13, and the fact that the volume fraction of stress induced martensite is lower at  $-196^{\circ}\text{C}$  than at  $-78^{\circ}\text{C}$  as shown in Fig. 12(b) and 12(c).

A correlation similar to that produced by a change in test temperature can be made by varying the stability with changes in composition or

with PDA temperature. The stress-strain curves for three steels of differing nickel contents, deformed 70 percent at 450°C and tested at -78°C, are shown in Fig. 14. Most of the key features in these curves have been previously discussed. However, the striking difference in behavior between the completely stable steel, CN16Cr, and the highly unstable one, CN8Cr, is worthy of note, as is the comparatively large elongation of steel, CN12Cr. As Tamura (36), Gerberich et al (3), and Bressanelli and Moskowitz (37) have observed, maximum elongation is produced in these steels when martensite is produced at an optimum rate with strain. Too little martensite per unit of strain fails to prevent necking and too much results in premature failure by fracture of the brittle martensite. The relatively low  $m$  value (estimated to be between 1.0 and 1.5) indicates that for steel CN12Cr the criterion for a large elongation to fracture has been met.

Changes in austenite stability can be induced by variations in the PDA temperatures, as shown earlier for both the carbonless Fe-Ni alloys and the carbon containing steels. The room temperature engineering stress-strain curves of steel, CN8Cr, deformed 70 percent at PDA temperatures of 200°, 250° and 450°C are shown in Fig. 15. The corresponding  $V_{\alpha}$  vs  $\epsilon$  curves are shown in Fig. 16 and the respective  $m$  values are indicated. The changes in stability produced by varying the PDA temperatures are reflected in both the mechanical properties and the transformation behavior. Several features are worthy of note. The variation of the yield strength with PDA temperature, with a maximum near 250°C, was discussed at length in an earlier section. The well defined (and small) Lüders strain and the high work hardening rate of the specimen deformed



at 450°C reflect its decreased stability, and these features are consistent with the data shown in Fig. 11.

Interrelationships - Stability, Properties, Processing, Testing

In the foregoing discussion an attempt was made to isolate and characterize some of the structural and chemical changes that are produced by variations in the processing and testing of high strength metastable austenitic steels. These changes and their effects on stability and mechanical properties were studied with emphasis on composition variations, PDA temperatures and test temperatures. Investigators have recently studied other aspects of these steels, such as (1) the role of stability in controlling fracture toughness and low cycle fatigue behavior, (2) the effects on mechanical properties of the amount and the time at temperature of deformation (PDA) and (3) the influence of strain rate on the tensile properties. References to these studies have been included in the bibliography. By using the information available from these studies it is possible to synthesize high strength steels with desired combinations of properties. Table III summarizes the general effects of compositional, processing and testing variables on both the stability and mechanical properties of these steels. Vertical arrows are used to indicate whether the stability or a mechanical property is increased (arrow up) or decreased (arrow down) by a corresponding change in a particular variable. In some cases a property may change in either direction, depending on particular circumstances. Whenever the effects of a particular variable are unknown, a question mark is shown. A brief discussion of some examples taken from Table III follows:

TABLE III

Probable Relationships Between Stability, as Affected by Several Processing and Testing Variables, and Selected Mechanical Properties

Variable	Stability	Mechanical Property					
		Yield Strength	Lüders Strain	Elongation	Work Hardening Rate	Fracture Toughness	Resistance to Hydrogen Embrittlement
COMPOSITION (increasing)							
Substitutional solutes (exception of Co)	† (3,23)	† (23)	† (3,23)	††(3,23)	† (23)	† (10)	† (41-43)
Interstitial solutes (C and N)	† (3-5,23)	† (4,5,23)	† (3-5,23)	††(3-5,23)	† (4,5,23)	† (10)	††(41-43)
PROCESSING (All variables increasing)							
Amount of deformation (PDA)	† (3)	† (3,5,23)	† (3,5,23)	††(2,3,5,23)	† (2,5,23)	† (10)	† (41-43)
Temperature of deformation (PDA)	††	††	††	††	††	†† (10)	††(41-43)
Time at temperature of deformation (PDA)	† (39)	† (39)	† (39)	††(39)	† (39)	?	† (41-43)
TESTING							
Test Temperature (decreasing)	†(3-5)	††(3-5)	††(3-5)	††(3-5)	††(3-5)	††(6,7,10)	††(40-43)
Strain Rate (increasing)	† (37)	††(37)	††(37)	††(37)	††(37)	††(6,7,10)	††(40-43)

Note: ( ) refers to relevant paper in the bibliography.

An increase in the alloy content of a steel will, in virtually all cases (with the possible exception of Co), increase the stability, but this is true only when the elements remain in solution in the austenite. An increase in stability can result in either an increase or decrease in elongation. The elongation is high for values of  $m$  between about 0.5 and 1.0, as was shown in Fig. 11(b). Below 0.5 the martensite produced per unit strain is small and therefore the rate of work hardening is too low to prevent necking, and above about 1.0 the elongation decreases with decreasing stability because the large amount of martensite produced per unit strain leads to brittle failure. In general, decreasing the stability by changes in composition results in higher levels of fracture toughness (10). For example, a steel with an  $m$  value of about two exhibited a  $K_{Ic}$  of 450,000 psi-in<sup>1/2</sup>. A further decrease in stability would probably have resulted in a lower fracture toughness because of the brittle fracture of the large amounts of strain induced martensite produced at the crack front (38).

Sauby, in unpublished work, has shown that aging thermomechanically processed "stable" austenitic steels can result in a decrease in stability and a corresponding increase in elongation with little loss in strength (39). The effective aging temperature was at or above the PDA temperature. Another interesting property of metastable austenitic steels is their resistance to hydrogen embrittlement (40-42).

Several other properties of high strength metastable austenitic steels have been studied which were not included in Table III. These include the corrosion resistance (43), and the welding characteristics (44). In the latter, the stability is an extremely important factor.

SUMMARY

Largely by controlling a single parameter, stability, it is now possible to produce metastable austenitic steels having a wide variety of useful combinations of mechanical properties. In this study, attempts were made to isolate and characterize changes in stability by systematic variations in composition, processing history and test environment. The effects of these changes in stability on the mechanical properties were studied; initially, in carbonless Fe-Ni alloys, and, finally, in more complex carbon containing alloys.

The mechanical properties of a severely cold-worked alloy, 38N, stable with respect to either athermal or isothermal phase transformations under all conditions of processing, were measured to provide a basis for comparison with the more complex and less stable systems that were subsequently studied. A less stable alloy, 34N, exhibited significant stability and mechanical property changes when either processed (rolled) or tested below the  $M_d$  or the  $M_s$ . When tested at  $-196^\circ\text{C}$ , below both the  $M_s$  and the  $M_d$ , this cold-worked alloy exhibited an unusual combination of mechanical properties (relative to those at room temperature), i.e., a lower yield strength, a much higher rate of work hardening, and twice the elongation at fracture. The unique deformation mechanism of austenite associated with these properties was that of a stress induced transformation to martensite.

At a test temperature ( $-78^\circ\text{C}$ ) between the  $M_d$  and the  $M_s$ , the mechanism of austenite deformation (of a cold-worked alloy, 34N) included both the stress and the strain induced modes. A stabilizing effect was

produced by deforming at higher PDA temperatures, which led to an accentuation of the strain induced mode. Progressive changes in the stress-strain curves of specimens processed with increasing PDA temperatures reflected the change in the mode of transformation. These results strongly suggested that the stability, the mode of transformation, and the mechanical properties of a carbonless metastable austenitic alloy can be changed by thermomechanical processing.

The behavior of the carbon containing alloys was, in many ways, analogous to that of the carbonless Fe-Ni alloys. However, in addition to the structural changes, chemical changes that affected austenite stability were evidently involved. Although the behavior of these steels was more complex, this disadvantage was somewhat offset by the fact that it was possible to follow, continuously and quantitatively by means of a magnetic technique, the course of the transformation with strain. Some of these observations are summarized below.

1) A maximum in the yield strength of all carbon containing fully austenitic alloys was observed for specimens processed at PDA temperatures between 200° and 300°C. The combined electron microscopy, magnetic and mechanical property evidence was consistent with the assumption that the maximum was due to the formation of carbon atmospheres around dislocations in the highly deformed matrix.

2) Two equations, proposed as quantitative descriptions of the relation between the volume of austenite transformed and the strain, were compared using transformation data obtained on the carbon containing alloys. A parabolic relationship, viz.,  $V_{\alpha} = m\epsilon^{1/2}$ , was found to be superior, particularly at large strains, to the autocatalytic form.

3) The relationship between stability and mechanical properties, using the stability coefficient  $m$ , was discussed for steels whose stability was varied by systematic changes in test temperature (22° to -196°C), composition (8, 12, 16 and 21 percents of Ni) and PDA temperature (25° to 450°C).

4) Studies of the shape of the  $V_{\alpha}$  (volume of austenite transformed) vs  $\epsilon$  (conventional strain) curves, coupled with a detailed examination of the features of the stress-strain curves of several steels, permitted unambiguous characterization of the stress induced mode of transformation of austenite.

5) Lastly, a summary in tabular form was made of predominant effects of compositional, processing and testing variables on the mechanical properties of ultra high strength metastable austenitic steels.

ACKNOWLEDGMENTS

The authors wish to express their deep appreciation to Dr. W. W. Gerberich and Professor G. Thomas for many helpful discussions.

This work was performed under the auspices of the United States Atomic Energy Commission through the Inorganic Materials Research Division of the Lawrence Berkeley Laboratory at the University of California, Berkeley, California.

REFERENCES

1. V. F. Zackay, E. R. Parker, D. Fahr and R. Busch: Trans. ASM, 1967, vol. 60, p. 252.
2. J. A. Hall, V. F. Zackay and E. R. Parker: Trans. ASM, 1969, vol. 62, p. 965.
3. W. W. Gerberich, G. Thomas, E. R. Parker and V. F. Zackay: Proc. Second Intern. Conf. on the Strength of Metals and Alloys, Asilomar, Calif., August 1970, p. 894.
4. G. R. Chanani, V. F. Zackay and E. R. Parker: Met. Trans., 1971, vol. 2, p. 133.
5. D. Fahr: Met. Trans., 1971, vol. 2, p. 1883.
6. W. W. Gerberich, P. L. Hemmings, M. D. Merz and V. F. Zackay: Trans. ASM, 1968, vol. 61, p. 843.
7. W. W. Gerberich, P. L. Hemmings, V. F. Zackay and E. R. Parker: Fracture 1969, ed. P. L. Pratt, p. 288, Chapman and Hall Ltd., London, 1969.
8. W. W. Gerberich and J. P. Birat: Intern. J. Fract. Mechanics, 1971, vol. 7, p. 108.
9. S. D. Antolovich and B. Singh: Met. Trans., 1971, vol. 2, p. 2135.
10. W. W. Gerberich, P. L. Hemmings and V. F. Zackay: Met. Trans., 1971, vol. 2, p. 2243.
11. G. R. Chanani: D. Eng. Thesis, UCRL Report 19620, University of California, Berkeley, July 1970.
12. R. M. Bozorth: Ferromagnetism, D. Van Nostrand Co., New York, 1951.



13. K. Hoselitz: Ferromagnetic Properties of Metals and Alloys, Clarendon Press, Oxford, 1952.
14. E. Scheil: Z. Anorg. Allg. Chem., 1932, vol. 207, p. 21.
15. B. L. Averbach, S. A. Kulin and M. Cohen: Cold Working of Metals, ASM, 1949, p. 290.
16. S. A. Kulin, M. Cohen and B. L. Averbach: Trans. AIME, 1952, vol. 194, p. 661.
17. T. Angel: J. Iron Steel Inst. 1954, vol. 177, p. 165
18. B. Cina: J. Iron Steel Inst., 1954, vol. 177, p. 406.
19. C. J. Guntner and R. P. Reed: Trans. ASM, 1962, vol. 55, p. 399.
20. J. F. Breedis and W. D. Robertson: Acta Met., 1963, vol. 11, p. 547.
21. R. P. Reed and C. J. Guntner: Trans. TMS-AIME, 1964, vol. 230, p. 1713.
22. R. H. Richman and G. F. Bolling: Met. Trans., 1971, vol. 2, p. 2451.
23. D. Fahr: Ph. D. Thesis, UCRL Report 19060, University of California Berkeley, September 1969.
24. J. C. Shyne, V. F. Zackay and D. J. Schmatz: Trans. ASM, 1960, vol. 52, p. 346.
25. E. T. Stephenson and M. Cohen: Trans. ASM, 1961, vol. 54, p. 72.
26. D. Kalish, S. A. Kulin and M. Cohen: Metals Eng. Quart., 1967, vol. 7, p. 54.
27. D. Kalish and M. Cohen: Mater. Sci. Eng., 1970, vol. 6, p. 256
28. R. A. Busch: Ph. D. Thesis, UCRL Report 16585, University of California, Berkeley, January 1966.
29. V. F. Zackay, W. W. Gerberich, R. Busch and E. R. Parker: Proc. First Intern. Conf. Fracture, Sendai, Japan, 1966, p. 813.

30. V. Goel, R. Busch and V. F. Zackay: Trans. ASME, J. Basic Eng., 1967, vol. 89, p. 871.
31. E. W. Page: M. S. Thesis, UCRL Report 18244, University of California, Berkeley, June 1968.
32. E. R. Parker and T. H. Hazlett: Relation of Properties to Micro-structure, p. 30, ASM, 1954.
33. J. B. Austin and R. L. Rickett: Trans. AIME, 1939, vol. 135, p. 396.
34. F. R. Schwartzberg, S. H. Osgood, R. D. Keys and T. F. Kiefer: Cryogenic Materials Data Handbook, Tech. Documentary Report ML-TDR-64-280, August 1964.
35. E. B. Kula and T. S. DeSisto: Behavior of Metals at Cryogenic Temperatures, ASTM Spec. Tech. Publ. 387, Philadelphia, 1966, p. 3.
36. I. Tamura, T. Maki, H. Hato, Y. Tomota and M. Okada: Proc. Second Intern. Conf. on the Strength of Metals and Alloys, Asilomar, Calif., August 1970, p. 900.
37. J. P. Bressanelli and A. Moskowitz: Trans. ASM, 1966, vol. 59, p. 223.
38. W. W. Gerberich: University of Minnesota, Dept. of Chemical Engr. and Mater. Sci., Minneapolis, private communication.
39. M. E. Sauby: M. S. Thesis, UCRL Report 19678, University of California, Berkeley, September 1970.
40. E. Gold and T. J. Koppenaar: Trans. ASM, 1969, vol. 62, p. 607.
41. R. A. McCoy, W. W. Gerberich and V. F. Zackay: Met Trans. 1970, vol. 1, p. 2031.

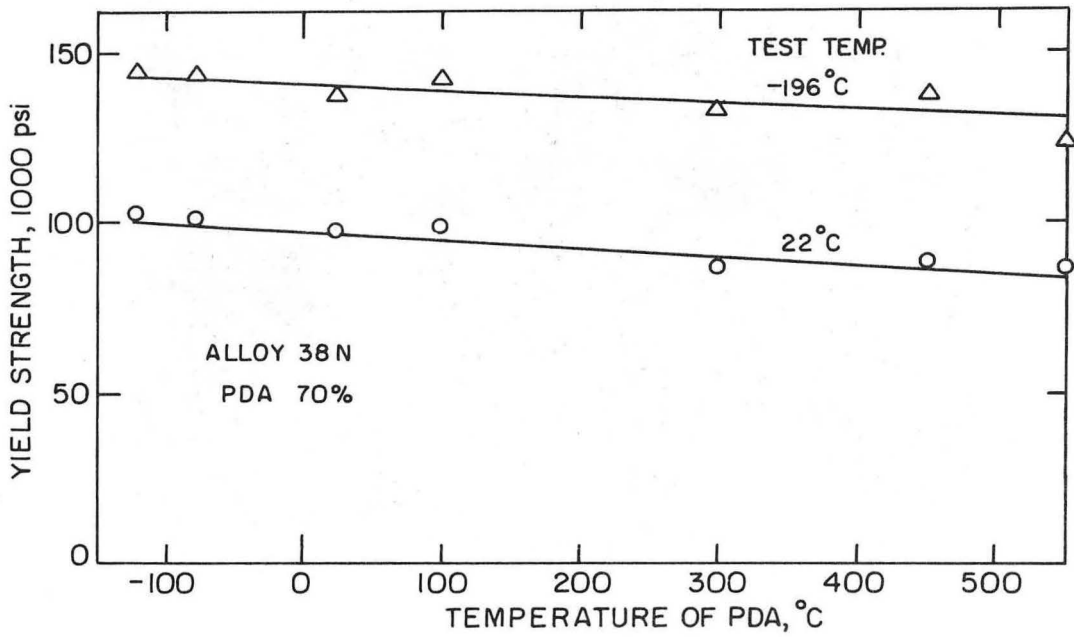
42. R. A. McCoy: D. Eng. Thesis, LBL Report 135, University of California, Berkeley, September 1971.
43. V. F. Zackay, W. W. Gerberich and S. F. Ravitz: Western Technical Conf., Los Angeles, Calif., March 1971 (V. F. Zackay and S. F. Ravitz are Professors, Dept. of Mater. Sci. and Engr., University of California, Berkeley; W. W. Gerberich is Associate Professor, Dept. of Chemical Engr. and Mater. Sci., University of Minnesota, Minneapolis).
44. S. M. Ambekar: D. Eng. Thesis, UCRL Report 19129, University of California, Berkeley, February 1970.

LIST OF FIGURES

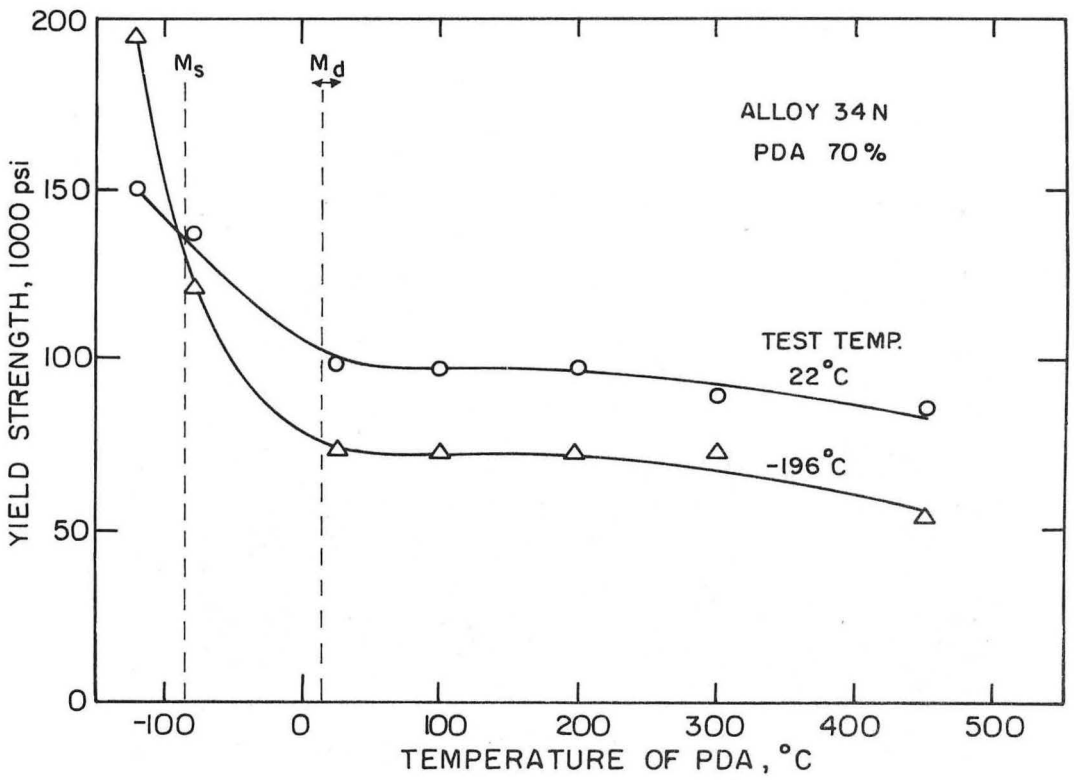
1. The effect of PDA temperature on the yield strengths of (a) alloy 38N, deformed 70 percent at the indicated temperatures (stable at all processing temperatures), and (b) alloy 34N, deformed 70 percent at the indicated temperatures (unstable below the  $M_d$ ).
2. Photomicrographs of specimens of alloy 34N, before testing: (a) rolled at a PDA temperature of  $-120^{\circ}\text{C}$ , showing martensite produced during rolling; (b) rolled above the  $M_d$  and cooled to  $-196^{\circ}\text{C}$ , showing the athermal martensite produced during cooling to the test temperature.
3. Typical engineering stress-strain curves for alloy 34N, at test temperatures of  $22^{\circ}$  and  $-196^{\circ}\text{C}$ , deformed 70 percent at a PDA temperature of  $450^{\circ}\text{C}$ .
4. The effect of PDA temperature on the yield strength of alloy 34N, deformed 70 percent and tested at  $22^{\circ}$  and  $-78^{\circ}\text{C}$ .
5. The engineering stress-strain curves of alloy 34N, deformed 70 percent at PDA temperatures of (a)  $25^{\circ}\text{C}$ , (b)  $200^{\circ}\text{C}$ , and (c)  $450^{\circ}\text{C}$ .
6. The effect of PDA temperature on the yield strength of steel CN28 at test temperatures of  $22^{\circ}\text{C}$  and  $-78^{\circ}\text{C}$ , deformed 70 percent at the indicated temperatures.
7. The effect of PDA temperature on the room temperature yield strengths of steels CN8Cr, CN12Cr, and CN21Cr, deformed 70 percent at the indicated temperatures.
8. The effect of PDA temperature on the  $-78^{\circ}\text{C}$  yield strengths of the steels shown in Fig. 7.

9. Transmission electron micrographs of a specimen of steel CN12Cr, deformed 70 percent at 300°C with (a) bright field image and SAD pattern, (b) dark field image using the  $(1\bar{1}1)_\gamma$  twin spot marked A in SAD, showing reversal of contrast at the twins.
10. The effect of PDA temperature for steel CN8Cr on the amount of martensite produced by strains of one and two percent.
11. The correlation between the stability coefficient,  $m$ , and (a) the Lüders strain, (b) the elongation to fracture for a large group of alloys of widely varying composition and processing histories (after Gerberich, et al, (3)).
12. The relation between strain and the volume fraction of martensite that is produced in steel CN8Cr, deformed 70 percent at 450°C, for test temperatures of (a) 22°, (b) -78°, (c) -196°C, and (d) -78°C and -196°C (after correcting for the fact that the volume fraction of stress induced martensite formed at -78°C was 0.15 greater than that formed at -196°C). The curves representing the relationship of  $V_\alpha$  and  $\epsilon$  suggested by Angel and Gerberich, et al, are also shown.
13. The engineering stress-strain curves of steel CN8Cr, deformed 70 percent at 450°C, at test temperatures indicated. The values of the stability coefficients,  $m$ , determined from the data of Fig. 12, are also shown.
14. The engineering stress-strain curves for three steels of differing nickel content (8 percent, 12 percent and 16 percent), deformed 70 percent at 450°C and tested at -78°C. The values of the stability coefficients,  $m$ , are shown.

15. The room temperature engineering stress-strain curves of steel CN8Cr, deformed 70 percent at PDA temperatures of 200°, 250° and 450°C. The values of the stability coefficients,  $m$ , are shown in Fig. 16.
16. The effect of strain on the volume fraction of martensite, at room temperature for steel CN8Cr, deformed 70 percent at PDA temperatures of (a) 200°, (b) 250° and (c) 450°C. The values of the stability coefficients,  $m$ , are shown.



(a)



(b)

XBL 7110-7490

Fig. 1.

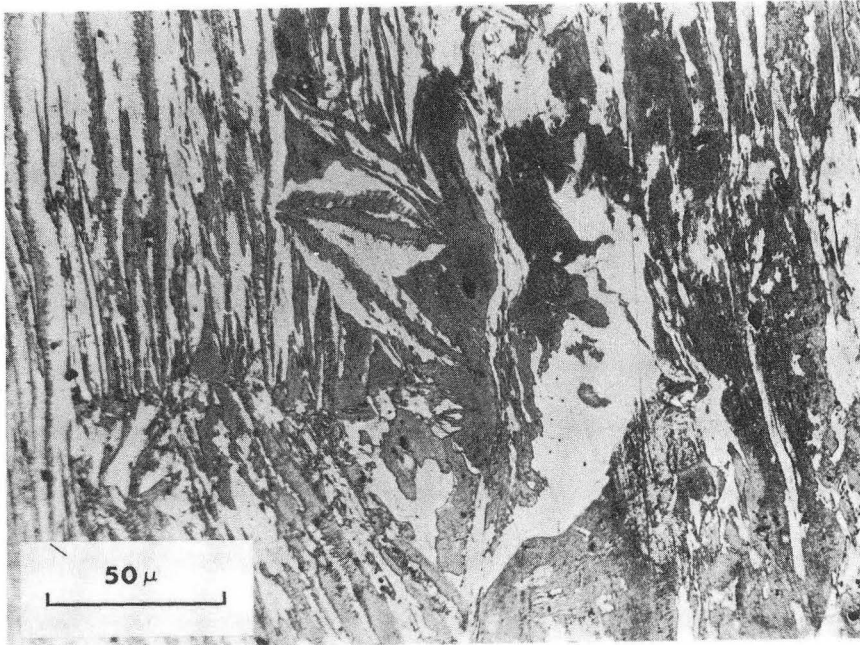
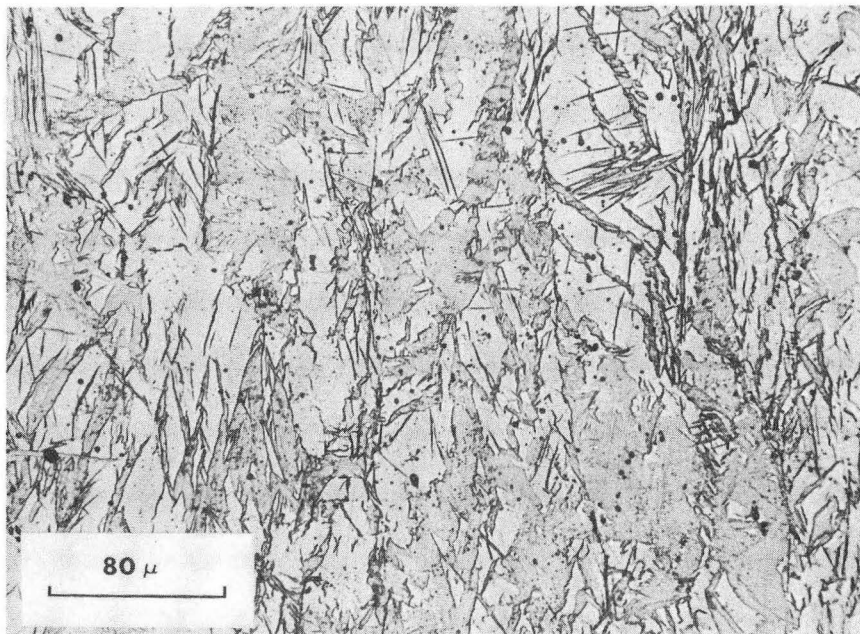


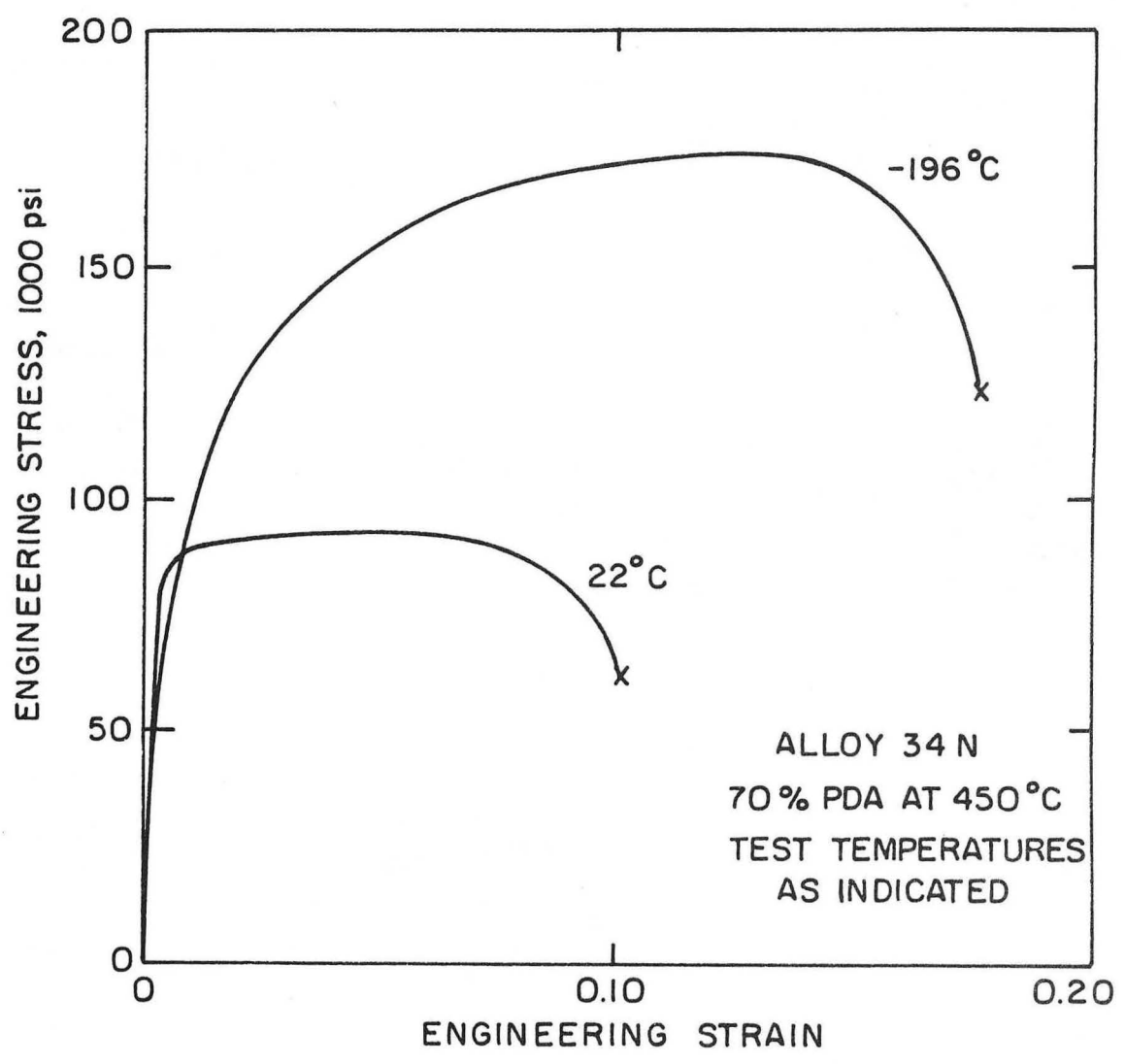
Fig. 2(a)



XBB 7111-5605

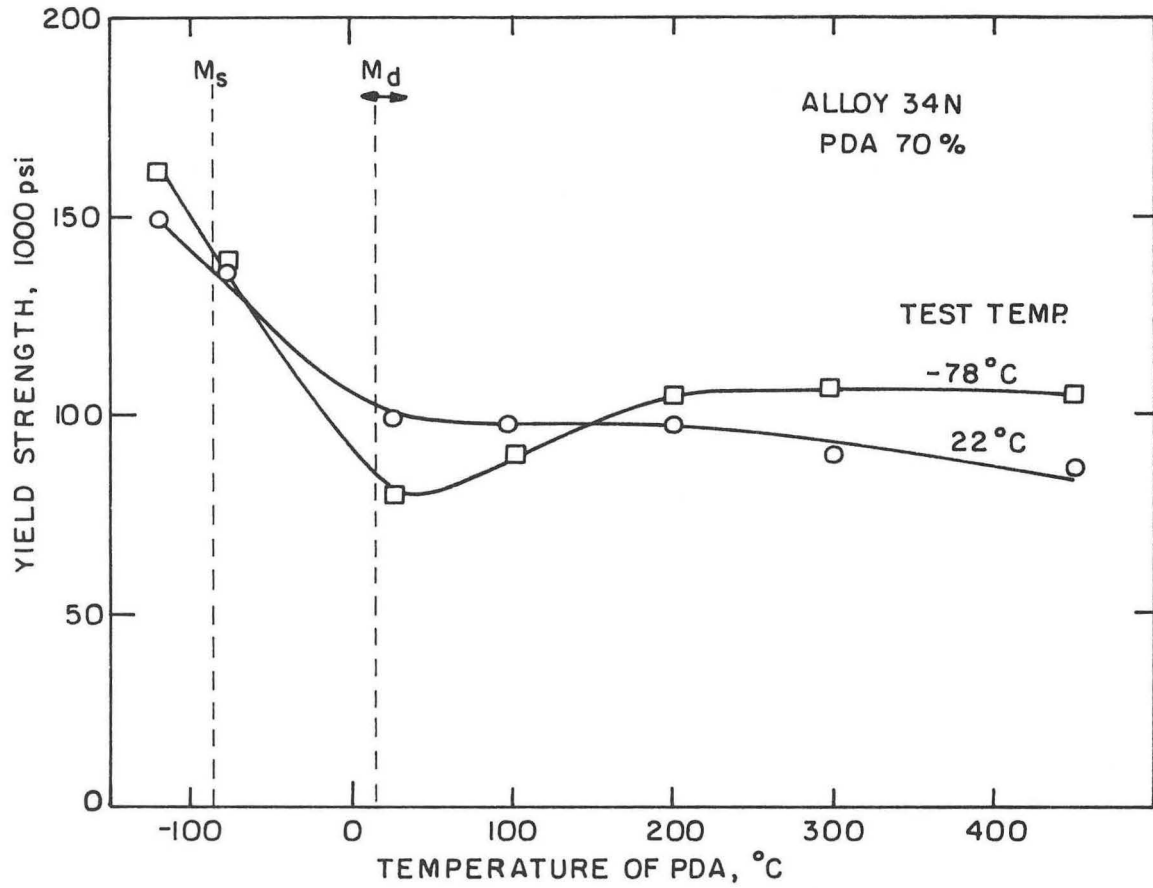
Fig. 2(b).





XBL 7110-7491

Fig. 3.



XBL 7110-7492

Fig. 4.

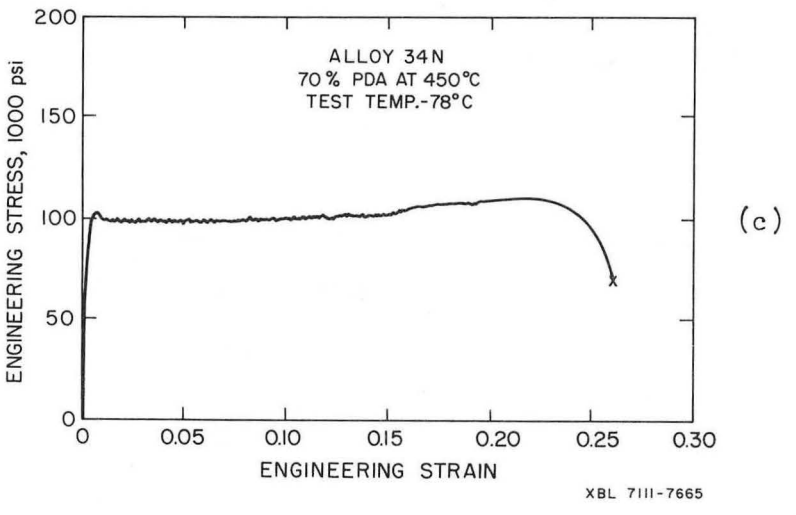
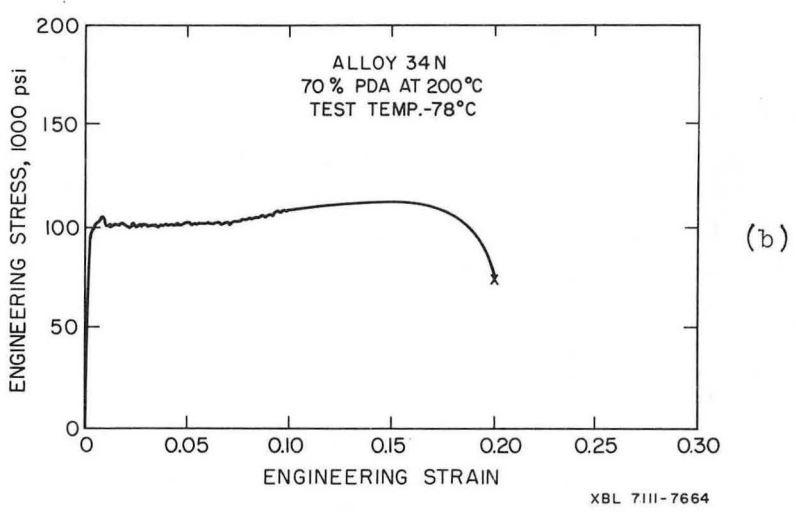
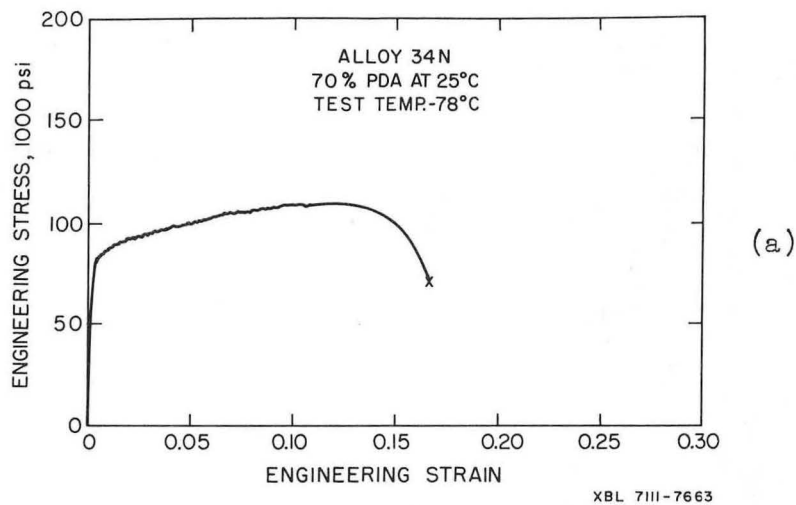
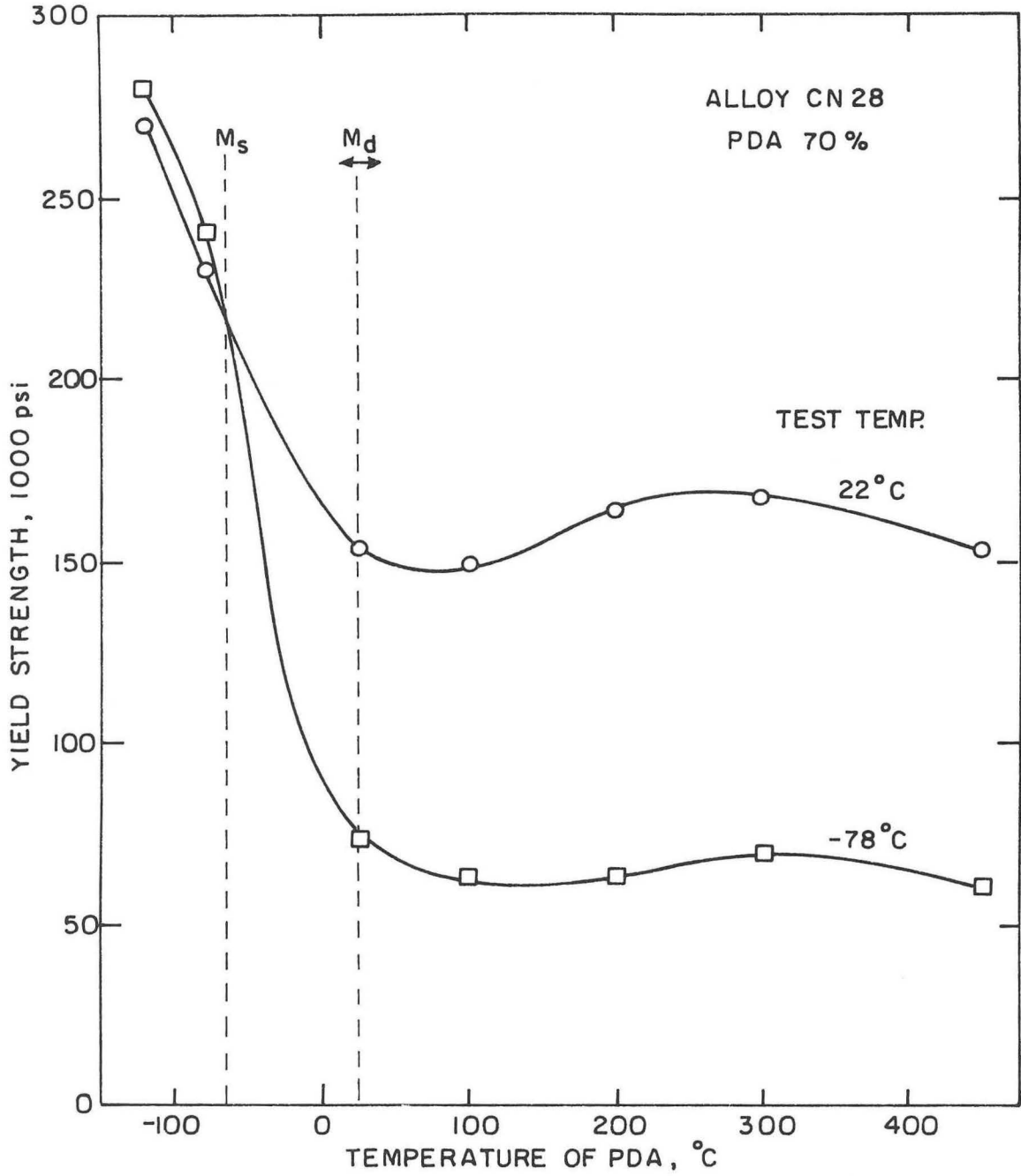
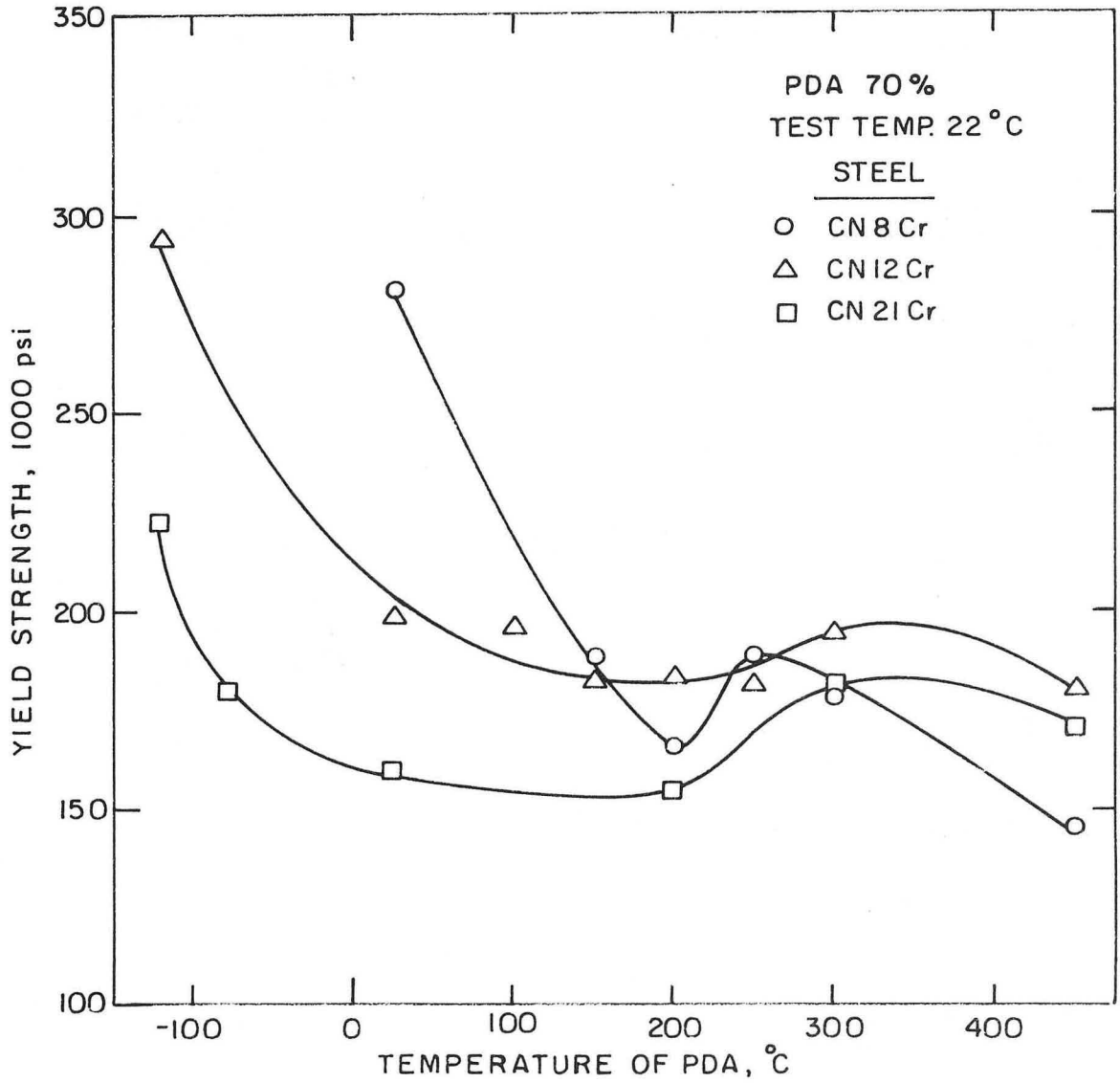


Fig. 5.



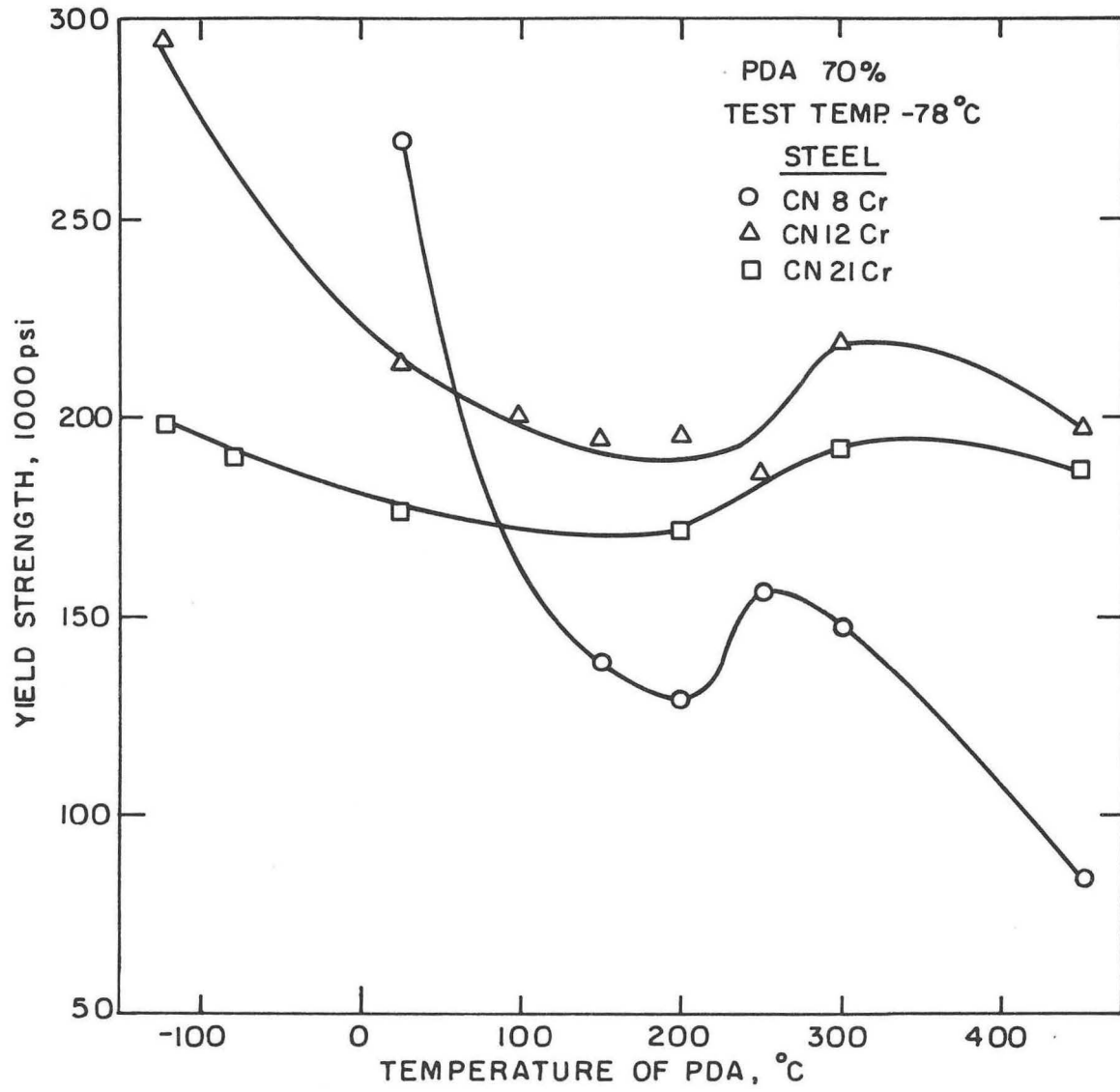
XBL 7110 7496

Fig. 6.



XBL 7110-7497

Fig. 7.



XBL 7110-7498

Fig. 8.

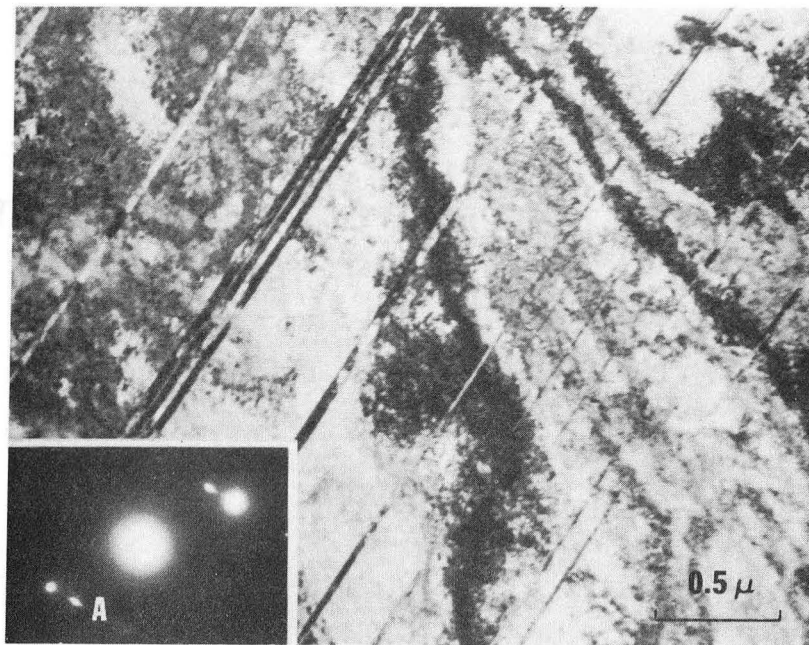
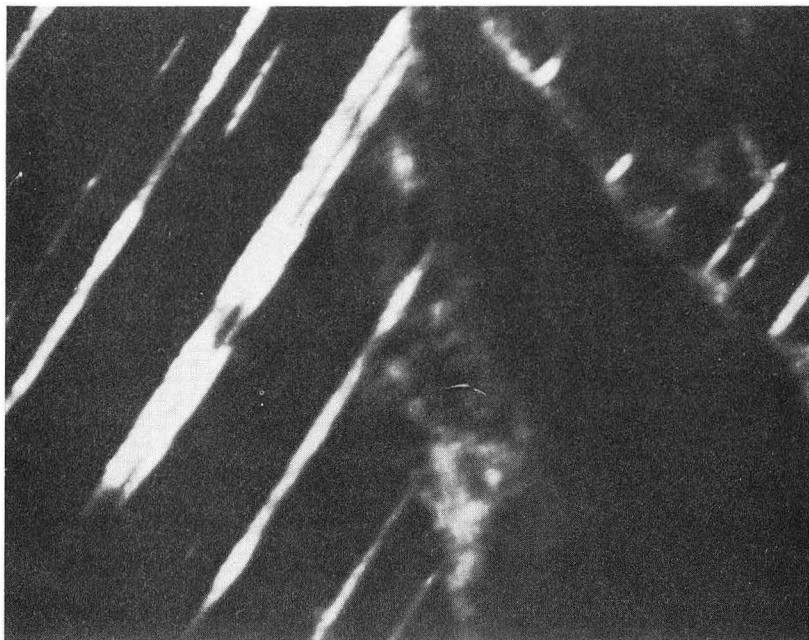
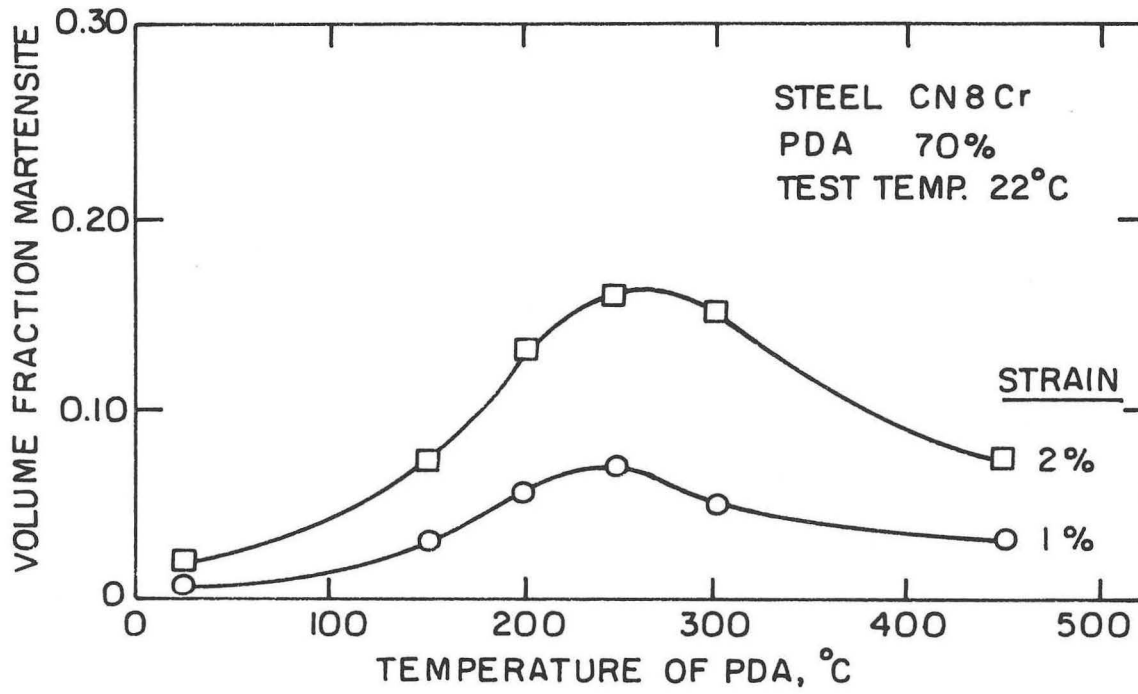


Fig. 9(a).



XBB 7111-5607

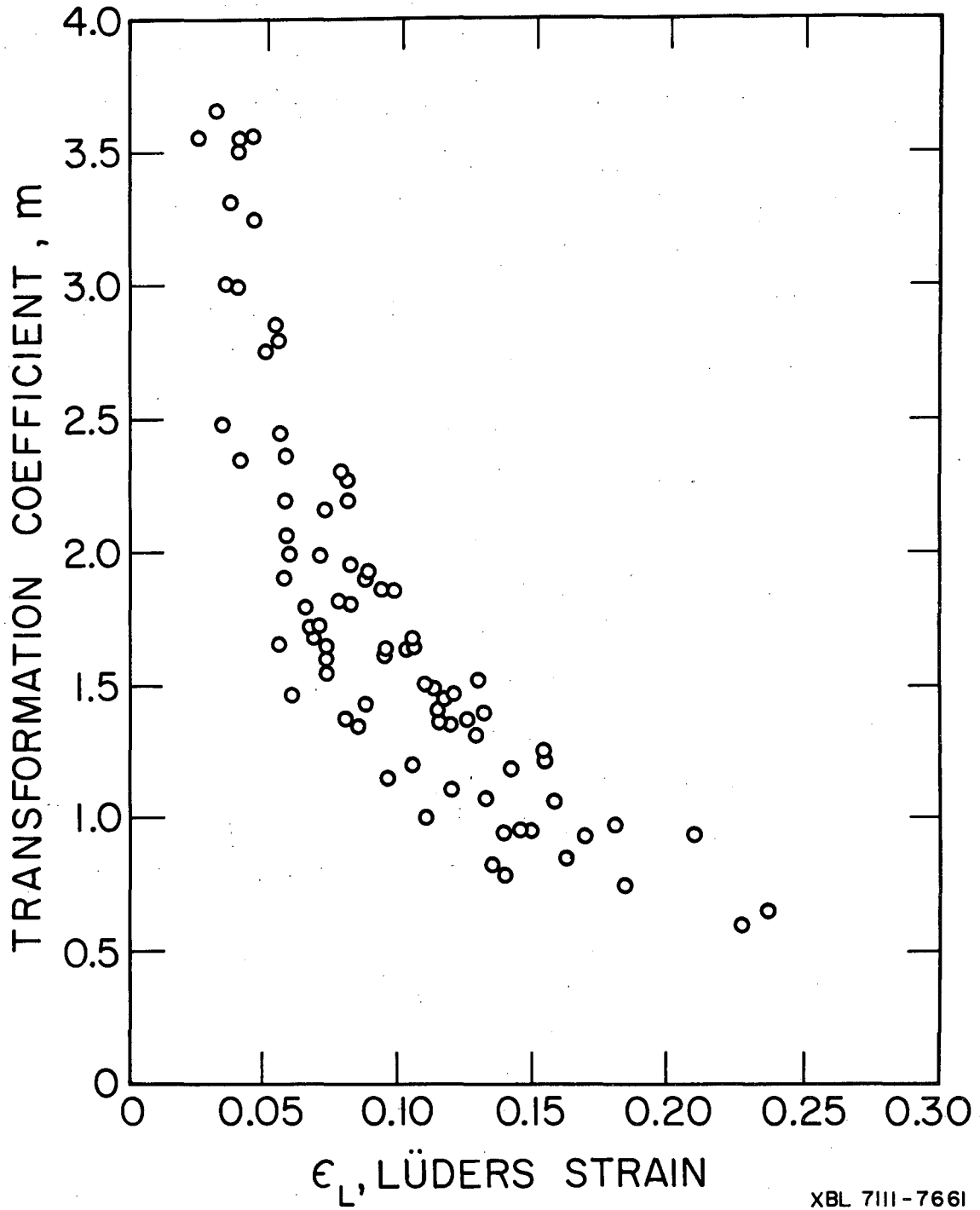
Fig. 9(b).



XBL 7110-7499

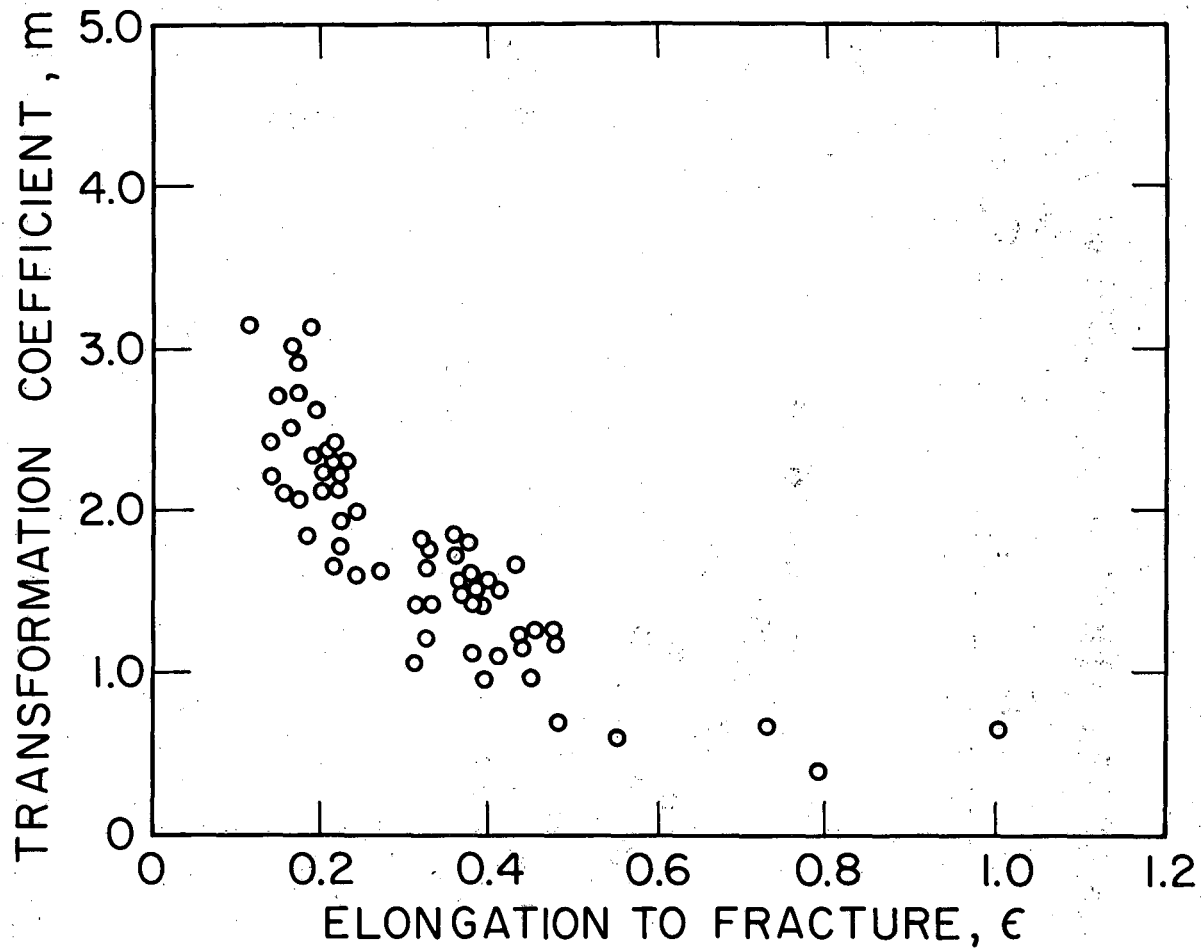
Fig. 10.





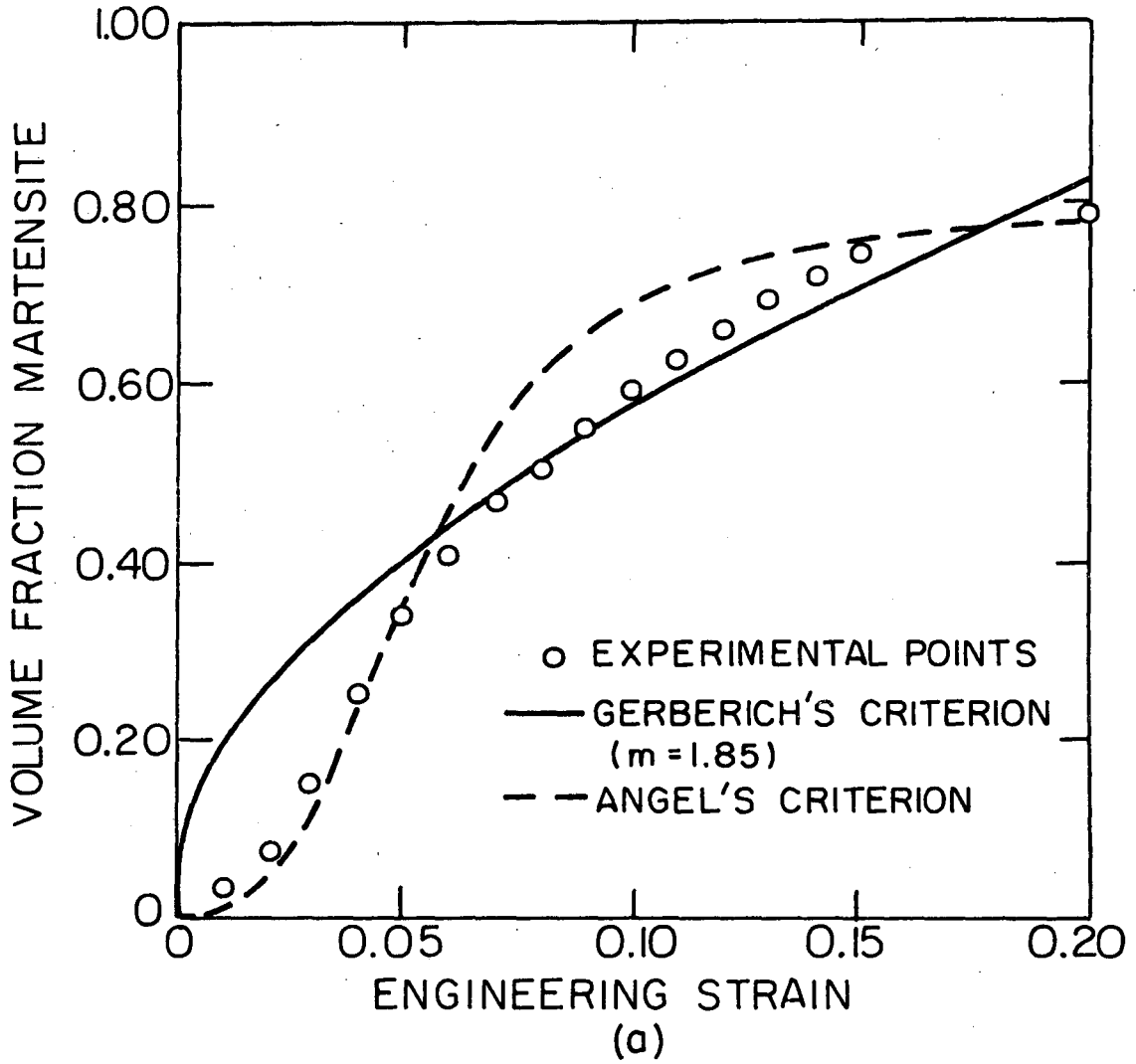
XBL 7111-7661

Fig. 11(a).



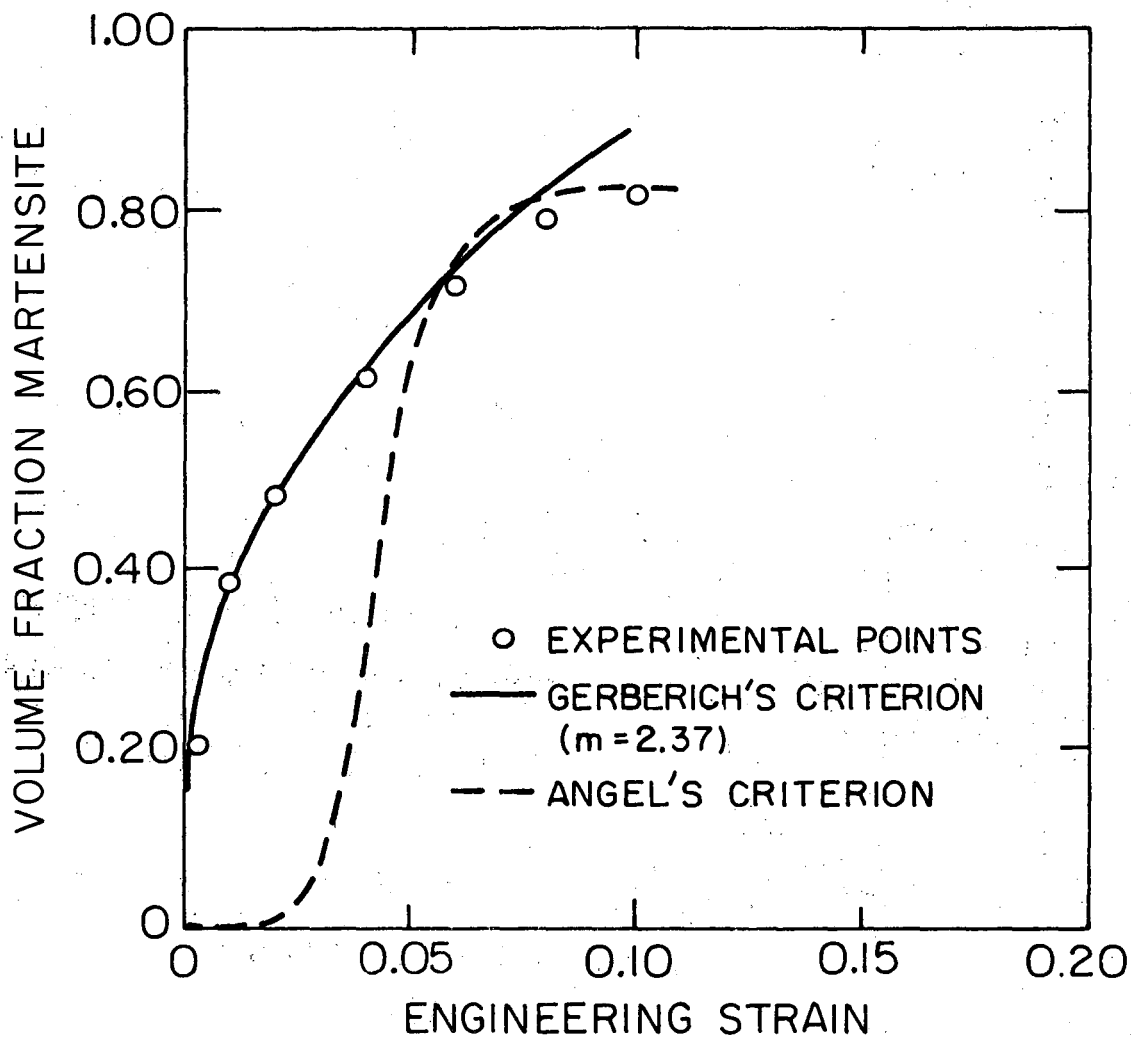
XBL 7HI-7662

Fig. 11(b).



XBL 7110-7500

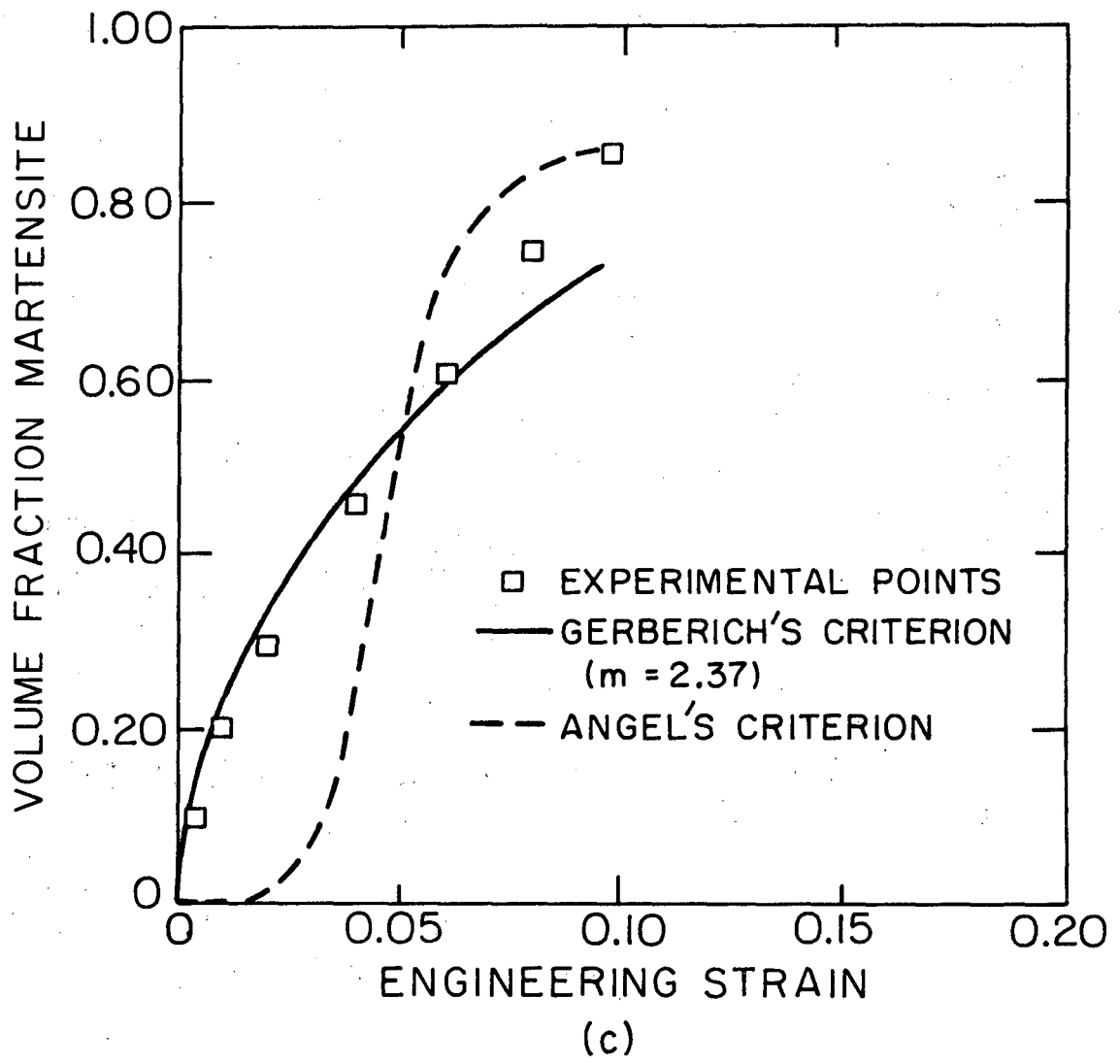
Fig. 12.



(b)

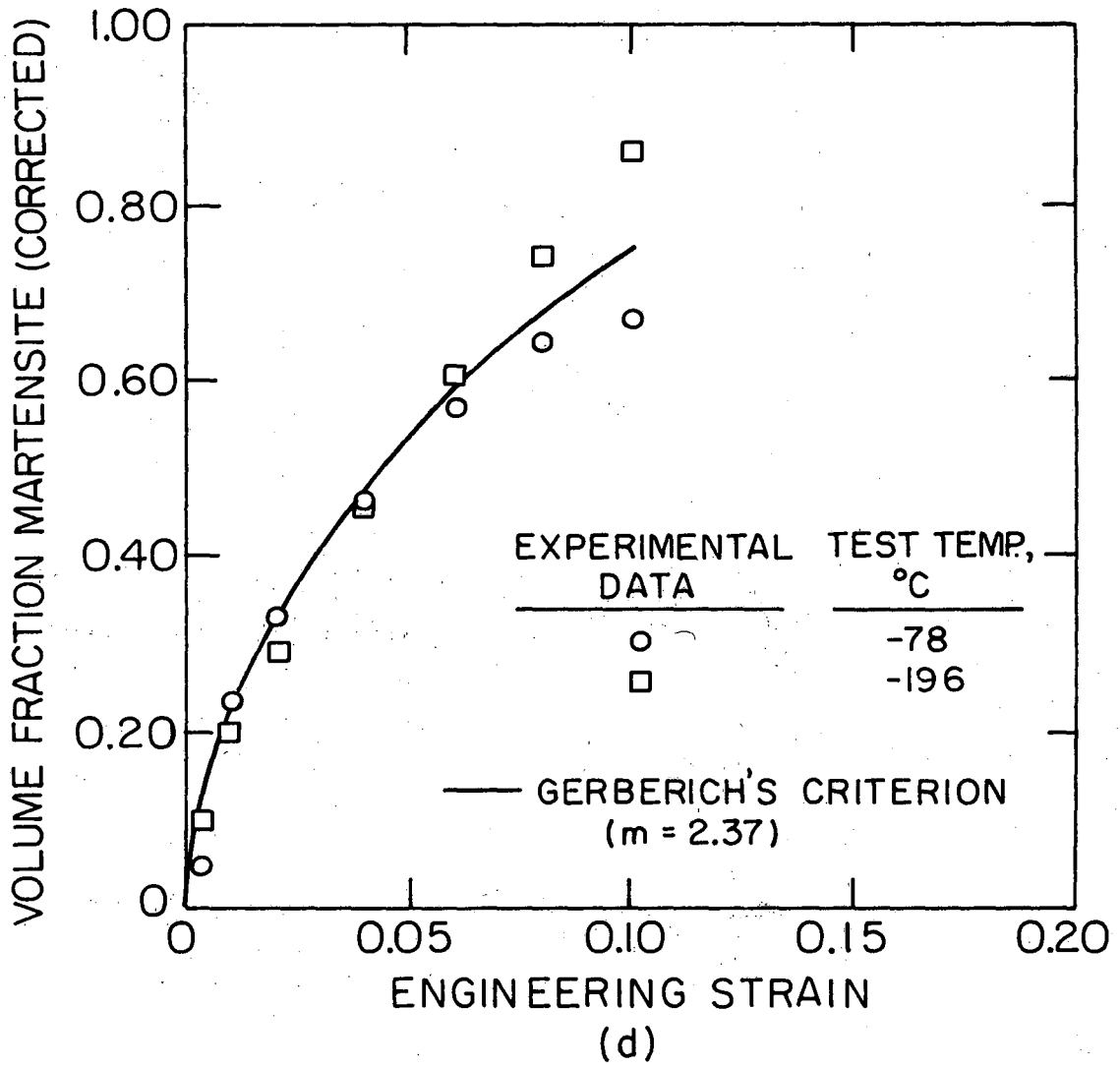
XBL7110-7501

Fig. 12.



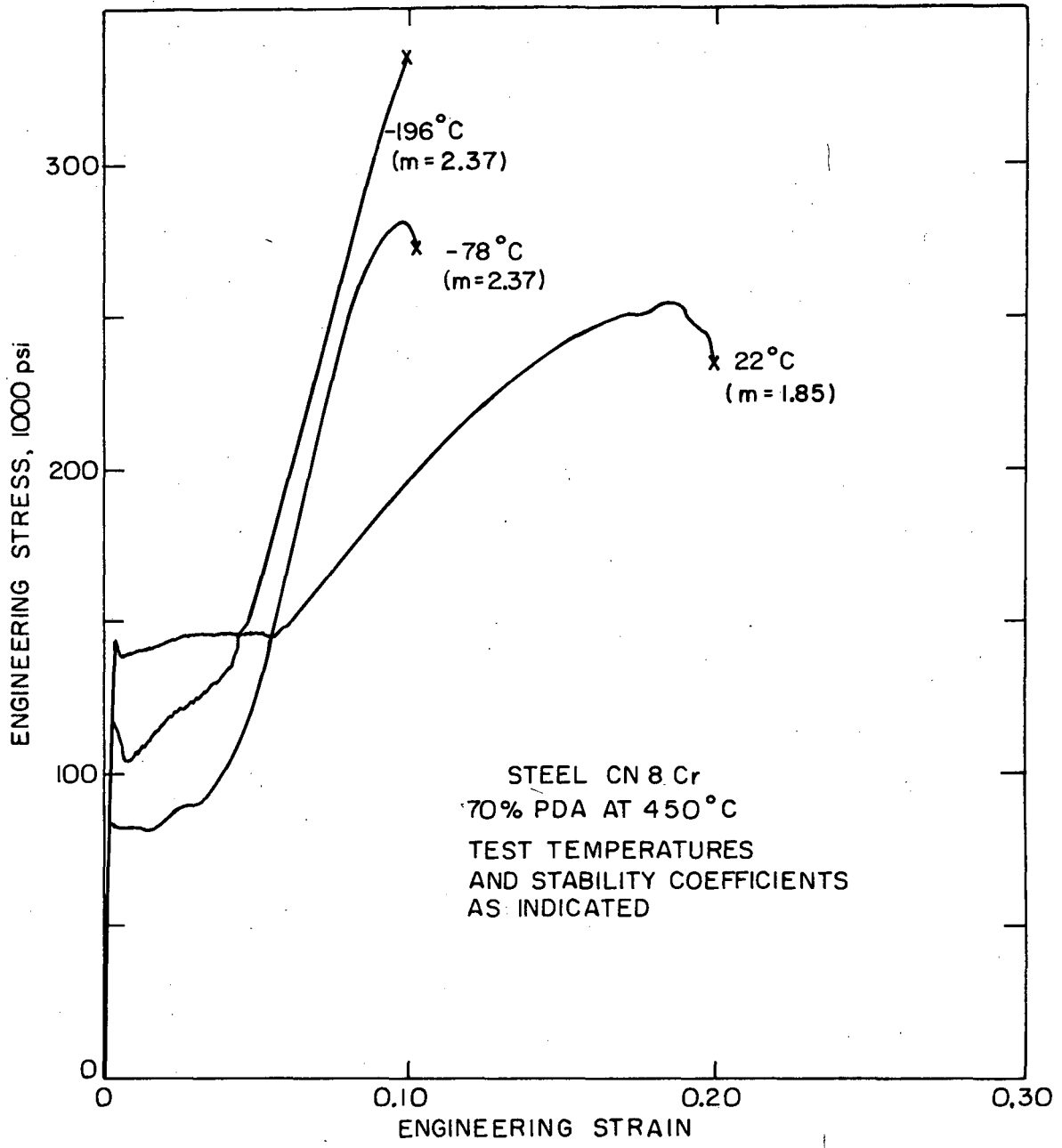
XBL 7110-7502

Fig. 12.



XBL 7110-7503

Fig. 12.



XBL 7110-7504

Fig. 13.

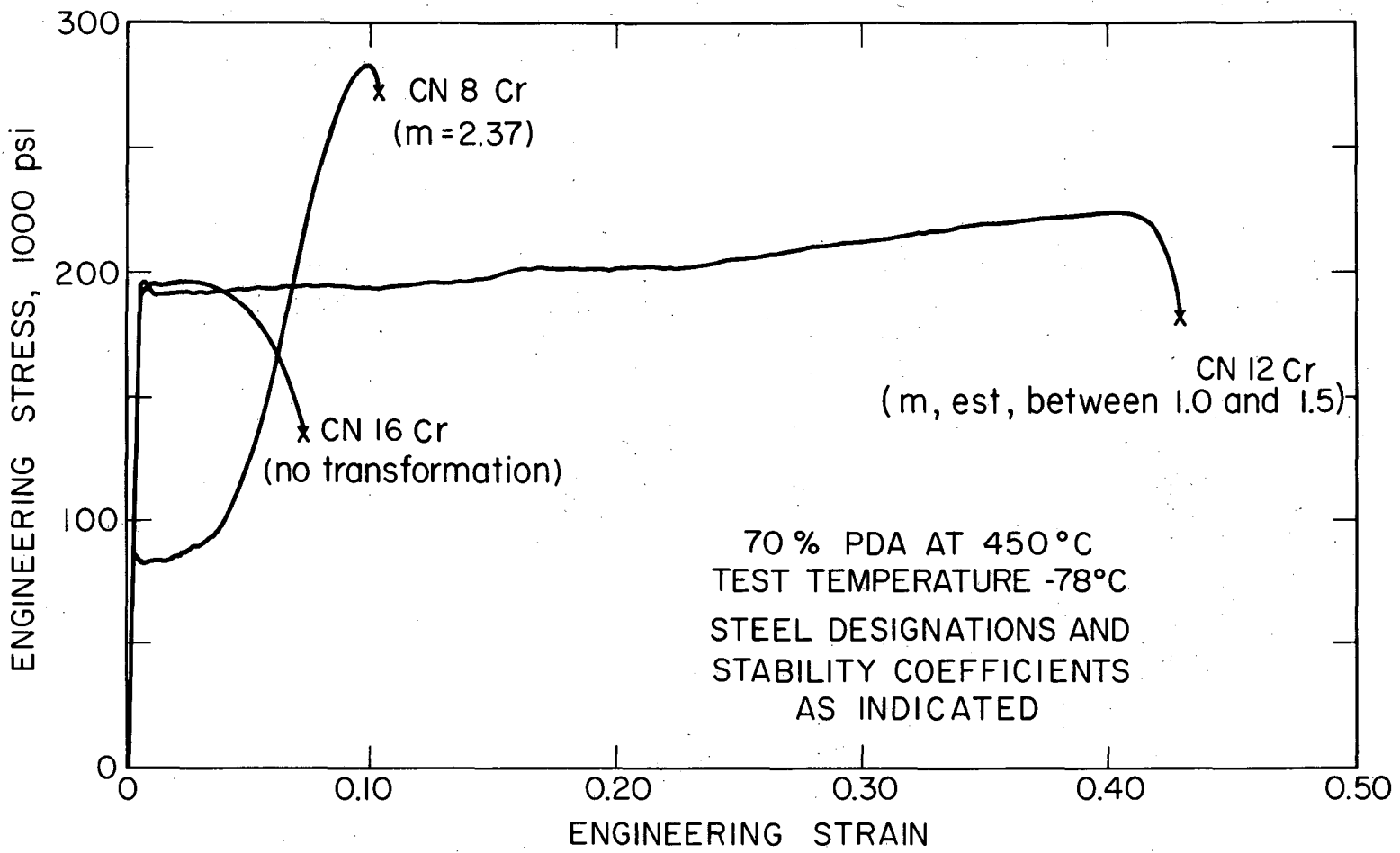
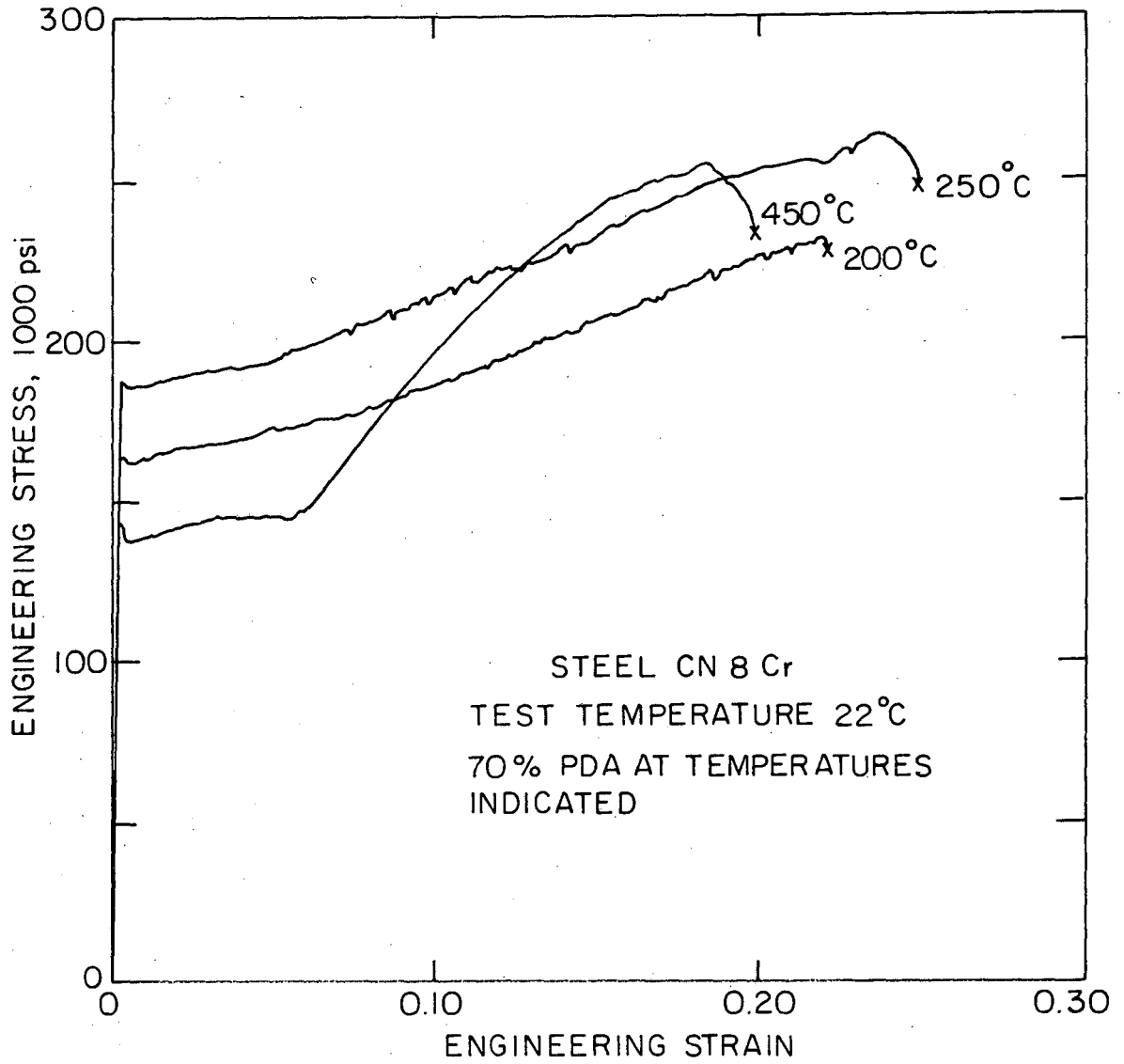


Fig. 14.

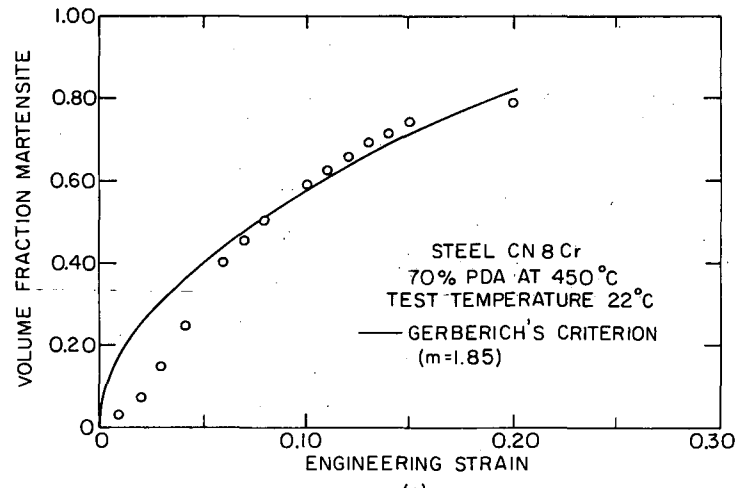
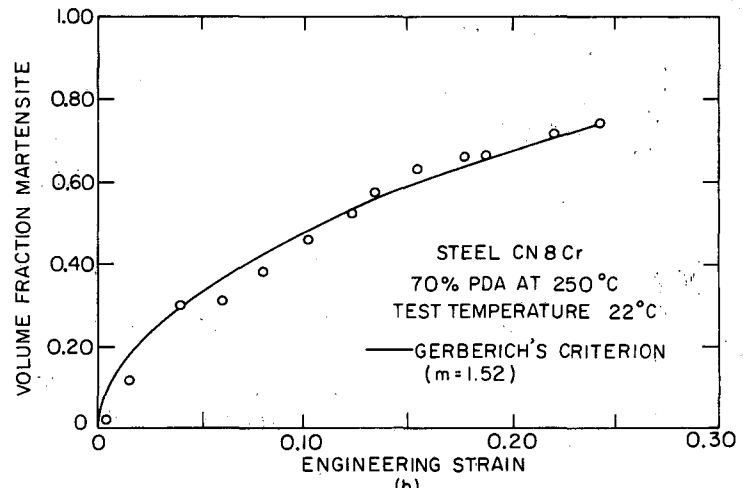
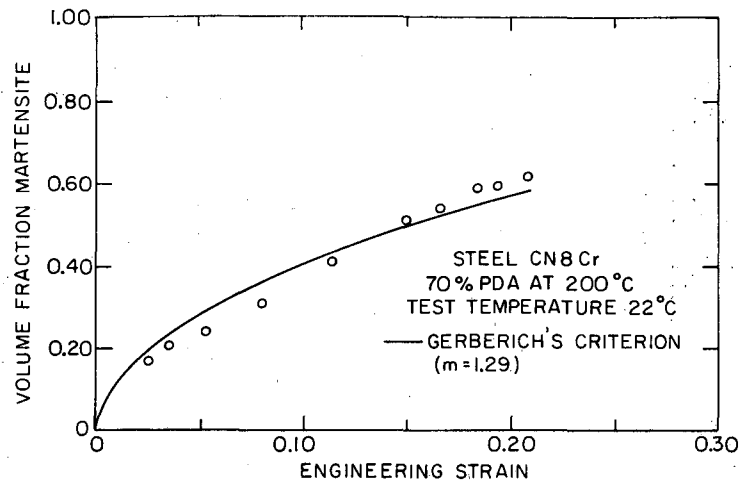
XBL 7111-7666





XBL 7110-7506

Fig. 15.



XBL 7110-7507

Fig. 16.

U S S O S S O S : 2 J

LEGAL NOTICE

*This report was prepared as an account of work sponsored by the United States Government. Neither the United States nor the United States Atomic Energy Commission, nor any of their employees, nor any of their contractors, subcontractors, or their employees, makes any warranty, express or implied, or assumes any legal liability or responsibility for the accuracy, completeness or usefulness of any information, apparatus, product or process disclosed, or represents that its use would not infringe privately owned rights.*

TECHNICAL INFORMATION DIVISION  
LAWRENCE BERKELEY LABORATORY  
UNIVERSITY OF CALIFORNIA  
BERKELEY, CALIFORNIA 94720